Theory, Substantiation, and Properties of Novel Reversible Electrocatalysts for Oxygen Electrode Reactions

ARTICLE *in* THE JOURNAL OF PHYSICAL CHEMISTRY C · MAY 2015

Impact Factor: 4.77 · DOI: 10.1021/jp510234f

5 AUTHORS, INCLUDING:

M. M. Jaksic

University of Belgrade

100 PUBLICATIONS **1,544** CITATIONS

THE JOURNAL OF PHYSICAL CHEMISTRY C

Review Article

pubs.acs.org/JPCC

Theory, Substantiation, and Properties of Novel Reversible Electrocatalysts for Oxygen Electrode Reactions

Jelena M. Jaksic,*[,†] Feihong Nan,[‡] Georgios D. Papakonstantinou,[†] Gianluigi A. Botton,[‡] and Milan M. Jaksic[†,§]

[†]Institute of Chemical Engineering Sciences, FORTH, GR-26504 Patras, Greece

[‡]Department of Materials Science & Engineering, McMaster University, 1280 Main Street West, Hamilton, Ontario L8S 4M1, Canada

[§]Faculty of Agriculture, University of Belgrade, 11030 Belgrade, Serbia

ABSTRACT: Hypo-d−(f)-oxides of transition elements ($d \leq 5$) usually feature decisive and highly pronounced effects of spontaneous adsorptive dissociation of water molecules, as the main and initial thermodynamic precondition state for the reversible latent storage and spillover properties of primary oxides (Pt−OH, Au−OH), otherwise indispensable ingredients in electrocatalysis for the oxygen electrode reactions. The higher the altervalent number (or capacity) of the former, and when mostly further advanced for the proper mixed valence hypo-d−(f)-oxide supports, the higher the overall (electro)catalytic yields primarily for cathodic oxygen reduction (ORR) and its anodic evolution (OER). In fact, cyclic voltammetry revealed the interrelated redox properties of the primary (Pt−OH) and surface (Pt═O) oxides between the cathodic hydrogen and anodic oxygen evolving limits, though the former has already been for longer known as the intermediate state from hydrogen oxidation in heterogeneous Doeberriner reaction upon Pt catalyst, and as being water molecules self-catalyzed (Ertel). Such interfering interrelated and autocatalytic species substantially define electrocatalytic properties of plain (Pt) or noninteractive supported noble metals (Pt/C), along the potential axis, and within some range even make them highly polarizable. Meanwhile, the latter can be continuously and successfully electrocatalytically depolarized and maintained reactivated. Such spontaneously renewable activation and maintenance of the reversible electrocatalytic state for the oxygen electrode reactions all along such cyclic voltammograms is the main Sir William Grove target challenge of the present study. In such a respect, continuously and spontaneously renewable adsorptive water molecule dissociation effectively means and enables the latent storage and electrocatalytic spillover properties of the primary oxide(s) for the reversible oxygen electrode (ROE) behavior, and these have been identified and substantiated, back and forth, all along the potential axis between hydrogen and oxygen evolving limits. Such advanced electrocatalytic properties imply selective grafting of interactive (SMSI, strong metal−support interaction) nanostructured hyper-d-Pt (Au, RuPt) clusters upon individual and/or preferably composite mixed valence hypo-d−(f)-oxide supports. The latter then feature the extra high stability, pronounced electronic conductivity, and many other d-electronic-based metal properties mostly arising and being established upon the hypo−hyper-d−d−(f)-interelectronic bonding effect, along with and based upon spontaneous dissociative water molecule adsorption upon exposed oxide support surfaces, thereby yielding renewable primary oxide latent storage by simple continuous water vapor supply and imposed characteristic membrane type hydroxide ion surface migration. Migrating hydroxide, as individual species, under imposed polarization transfers its prevailing part of electron to the metallic electrocatalyst, hence resulting as the Pt−OH (Au−OH) dipole, and by the surface repulsion obeys reversible spillover distribution and imposes the electrocatalytic ROE properties all over the catalyst surface and DL pseudocapacitance charging and discharging, as well. The strong adsorptive surface oxide (Pt═O → 1) deposition out of the primary oxide (Pt−OH → 0) irreversible disproportionation thereby imposes unusually high reaction *polarization* of Pt, Au, Pd, and all other noble and transition d-metals within a very broad (600 mV, and even broader) potential range and, thereby, in general, mostly pronounced polarizable noncatalytic properties for oxygen electrode (ORR, OER) reactions. Thus, the strong interactive and selective hypo−hyper-d−d-interelectronic grafting bonding of nanostructured individual (Pt) or prevailing hyper-d-intermetallic phase ($MoPt_3$; $HfPd_3$) cluster catalysts on altervalent and mixed-valence hypo-d−(f)-oxide supports, as

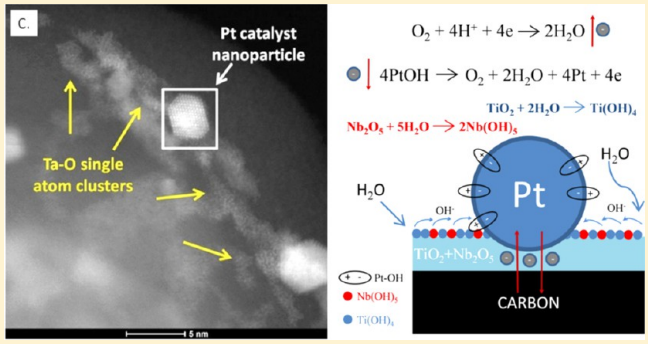

continued...

Received: October 11, 2014
Revised: February 27, 2015
Published: March 2, 2015

DOI: 10.1021/jp510234f
J. Phys. Chem. C 2015, 119, 11267−11285

substantially and typically based upon the metallic d−d- or d−f-interelectronic bonding strengths and SMSI features, provide and keep just inferred basically all (inter)metallic properties of composite electrocatalysts, the primary oxide latent storage, and enhanced spillover and thereby enable approaching their reversible (electro)catalytic properties and optimization for the ROE. The reversibly revertible alterpolar bronze behaves ($Pt/H_xNbO_5 \Leftrightarrow Pt/Nb(OH)_5$, $x \approx 0.3$) as the thermodynamic equilibrium alterpolar state, and thereby substantially advanced electrocatalytic properties of these composite interactive electrocatalysts for both oxygen (ORR, OER) and hydrogen (HOR, HER) electrode reactions, consequently, have been inferred as spontaneously altering and strong spillover features, in particular unique and superior for the revertible (PEMFC versus WE (water electrolysis)) cells.

INTRODUCTION

Ever since Sir William Grove[1] opened the field, invented, and proved the gaseous type fuel cells (FCs) concept and functional operation, reversible oxygen electrocatalysis has been the main imperative target, challenge, and dream of the entire electrochemical science. The latter has been primarily focused on noble (Pt, Au) metals, while the reversible primary (Pt−OH, Au−OH) and polarizable surface (Pt═O, Au═O) oxides, along with H-adatoms (Pt−H, Au−H), represent interactive species defining the overall electrode behavior and properties. The latter means and includes all redox occurrences between cathodic hydrogen and anodic oxygen evolving limits, revealed by corresponding peaks within cyclic voltammetry spectra. Meanwhile, these adsorptive hydrogen and oxygen species and their decisive electrocatalytic and/or polarizable effects belong to newer developments in electrochemical science, and while missing, the whole kinetic and catalytic knowledge and understanding for longer were obscure. In such a respect potentiodynamic spectra (Figure 1) usually reveal within a narrow potential range the highly reversible peaks of primary oxide adsorptive growth, along with self-catalytic stepwise molecular water oxidation and its backward desorptive removal[2,3]

$$Pt + 2H_2O \Leftrightarrow Pt{-}OH + H_3O^+ + e^- \quad (1)$$

as a typical double layer (DL) charging and discharging pseudocapacitance.[4−6] Meanwhile, the former sooner or later irreversibly disproportionates (Pt−OH → 0) into the strongly polarizable, more adsorptive, and more stable surface oxide (Pt═O → 1) monolayer[2,3]

$$Pt{-}OH + H_2O \Rightarrow Pt{=}O + H_3O^+ + e^- \quad (2)$$

with the corresponding pronounced irreversible desorption peak all along the equivalent reverse cathodic potential scan direction (Figure 1).

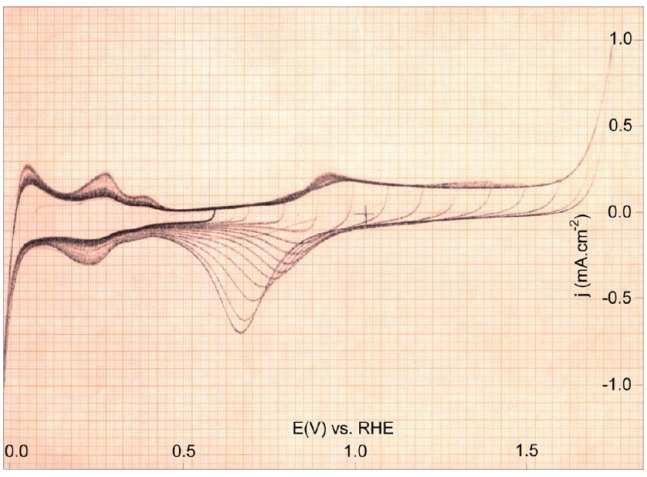

Figure 1. Cyclic voltammograms of polycrystalline Pt scanned in 0.1 M NaOH at a sweep rate of 100 $mV{\cdot}s^{-1}$.

The latter, in the absence of the Pt−OH, thereby imposes such a critical and typical, very pronounced reaction polarization range (Figure 1) (Pt−OH → 0, Pt═O → 1) all along until oxygen evolving potential limits and in both scan directions, back and forth.[4−6] Such a highly reversible (eq 1), relative to the subsequent strongly irreversible, and substantially polarizable (eq 2) transient has been decisive as concerns the overall electrocatalytic properties and behavior of both Pt and Au and all other plain noble and even many non-noble transition metal electrodes for the oxygen electrode reactions (ORR and OER). Meanwhile, while dealing with simple electrode reactions of cathodic hydrogen (and/or anodic oxidation) and anodic oxygen (and/or its cathodic reduction) evolution, researchers formerly omitted to reveal that the interrelation between the primary (Pt−OH) and surface (Pt═O) oxide defines the polarization properties of plain and noninteractive supported metal (Pt) catalyst.

Since the equimolar ratio of the primary and surface oxide concentrations defines the optimal interfering self-catalytic spillover reaction step in cathodic oxygen reduction (ORR),[7] or as the overall electrode reaction

$$Pt{-}OH + Pt{=}O + 3H_3O^+ + 3e^- \Rightarrow 5H_2O + 2Pt \quad (3)$$

and in particular along the reversible (low slope, 30 mV/dec, or even lower) parts of Tafel line plots, the irreversible disproportionation (eq 2) imposes an extremely high reaction *polarization barrier* (Pt−OH → 0, see later below) that amounts to even more than 600 $mV{\cdot}s^{-1}$ and then, in the absence of the Pt−OH spillover reactant, makes plain Pt (and Au) and noninteractive supported (Pt/C or Au/C) platinum and gold irreversible for the oxygen electrode reactions within the broader potential range, back and forth (Figure 1). The thermodynamic definition of irreversibility within the closed loop of reaction circles then would state that plain Pt(Au) by no means can feature the reversibility and/or (electro)catalytic activity all along the potential range in aqueous media. In other words, plain and noninteractive (Pt/C and/or Au/C) supported Pt(Au) electrodes themselves by no means can behave electrocatalytic features of the reversible oxygen electrode (ROE) all along the potential axis between hydrogen and oxygen evolving limits, back and forth. The strongly adsorptive and hence highly polarizable Pt═O (Au═O), deprived from any local and/or external Pt−OH (Au−OH) surface source and supply, then defines one of the most pronounced issues of the reaction *polarization* in the entire electrochemical science: No Pt−OH means that there is no reversible reaction (eq 3). Quite another story arises when the nanostructured Pt(Au) electrocatalyst is interactive selective grafting bonded on various, in particular mixed valence hypo-d−(f)-oxide, supports. Meanwhile, although interactive (SMSI) hypo-d−d-oxide supported catalysts (Pt) have already been broadly and successfully employed in heterogeneous catalysis, electrochemists still hesitated to employ them, mostly because of the expectancy for them to cause increasing IR drop and eventual chemical instability.

DOI: 10.1021/jp510234f
J. Phys. Chem. C 2015, 119, 11267−11285

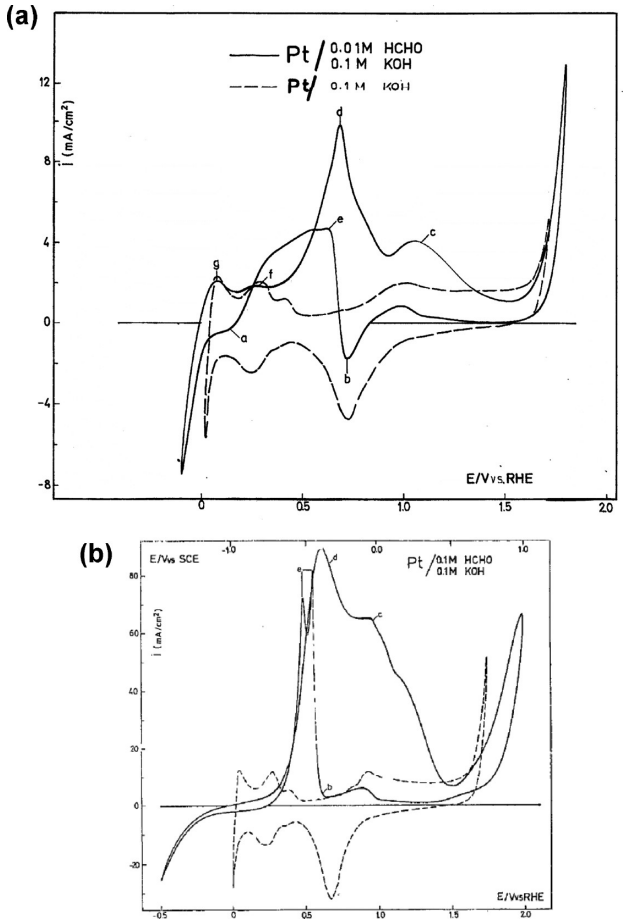

Figure 2. (a and b) Cyclic voltammograms scanned on a polycrystalline Pt wire electrode in alkaline (0.1 M KOH, dashed lines) solution and in an admixture of formaldehyde (0.01 M (a) and 0.1 M HCHO (b), full lines) at 200 mV·s^{-1} sweep rate between hydrogen and oxygen potential evolving limits. Labels: (a) reversible hydrogen adsorption peak; (b) irreversible Pt surface oxide (Pt═O) desorption peak; (c and d) successive peaks of anodic aldehyde oxidation; (e) sudden sharp anodic current jump and reverse hysteretic peak of repeated HCHO oxidation in the course of successive cathodic scan; (g and f) reversible H-adatom oxidation and desorption peaks, respectively.

The present analysis is best reflected and proved by comparison of Figure 1,2 and 3, once when missing Pt−OH spillover (Pt−OH → 0, Pt═O → 1), then when there proceeds simple effusion of self-generated Pt−OH, or finally, when enriched latent storage spillover enables enormous primary oxide adsorptive deposition and reverse desorption, (Pt−OH → 1, Pt═O → 0), exactly as big capacitors do, and when continuously and reversibly present all over the potentiodynamic cycle (see further downward detailed stepwise discussion). In such a respect, since potentiodynamic spectra reveal by corresponding peaks and their specific type and nature, all subtle redox occurrences in between of hydrogen and oxygen evolving limits, as the final and main products of electrode reactions, cyclic voltammetry represents the mine electrochemical analytical tool and system for characterization of all electrode events and their properties, in particular in electrocatalysis.

Electrocatalysis and Spillover Electrocatalysts for the ROE. Whereas hydrogen molecules undergo spontaneous adsorptive dissociation on plain Pt (Pt/C) yielding H-adatoms (Pt−H) to establish thermodynamic equilibrium of the RHE (reversible hydrogen electrode, (Pt(H_2)/Pt−H/H_3O^+)), within

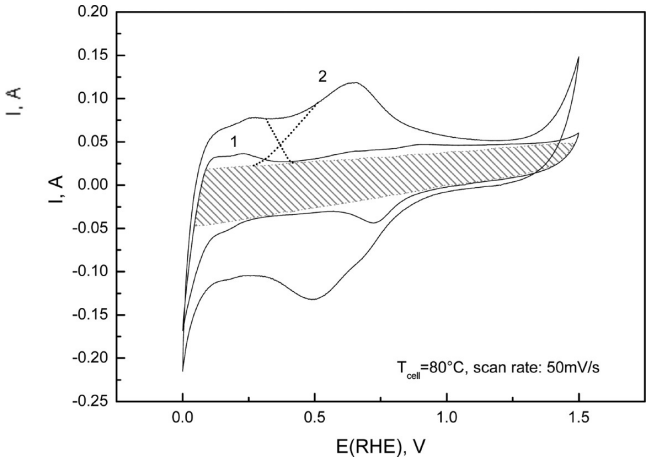

Figure 3. Cyclic voltammograms of an interactive (SMSI) supported nanostructured Pt electrode (Pt/TiO_2, WO_3/C), on mixed valence hypo-d-oxides, scanned in He stream, ones at negligible moisture content (curve 1) and at 80 °C water vapor saturation (curve 2).

the above identified critical reaction polarization potential range Pt(Au) is deprived (eq 2) from the Pt−OH (Au−OH) to provide establishing the reversible properties for the ROE ((Pt(O_2)/Pt−OH,Pt═O)/OH^-), and both together assemble the reversible hydrogen fueled L&MT PEMFCs. In other words, the Pt−OH (or Au−OH) plays the same thermodynamic constitutional role for establishing the equilibrium for the ROE as Pt−H does for the RHE and, hence, unavoidably imposes a continuous need and requires a permanent feeding source of the former (Pt−OH → 1) to overcome the reaction polarization (eq 2), by the latter (Pt═O → 0), and enables the reversible electrocatalytic properties of the ROE[5] (eq 3). In such a respect, the first main step in the present concept toward the ROE implies that catalytic hyper-d-metals (Pt, Au, Ru) establish with hypo-d−(f)-oxide catalytic supports (or advantageously their mixed valence compounds, like Nb_2O_5, TiO_2, CeO_2 or Ta_2O_5, TiO_2, CeO_2) the interactive Brewer type hypo−hyper-d−d−(f)-oxides (d−d or d−f) bonding effect,[8,9] otherwise well-known in heterogeneous catalysis as Tauster[10] SMSI (strong metal−support interaction), one of the strongest in all of chemistry (Figure 3, ref 4). Consequently, these interactive interbonded composite electrocatalysts (for example, Pt/Nb_2O_5, TiO_2), while strong bonding, impose remarkably stretched d-orbitals and thereby exhibit much weaker adsorptive interbonding strengths of intermediates (Pt−H, Pt−OH) in the RDSs (rate-determining steps), hence facilitating cleavage of the latter and increasing the (electro)catalytic activity for both hydrogen and oxygen electrode reactions. Meanwhile, some other accompanying effects, in particular the ones associated with the Pt−OH spillover, play an even more significant role for the latter (ROE). In such a respect, the dramatically pronounced Pt−OH spillover effect has primarily been noticed as the remarkably increased CO tolerance (Figure 7 in ref 4). First, hypo-d-oxides and their mixed valence compounds, as based on typical d−d−(f)-metallic bonds, exhibit extra high stability in both acidic and alkaline media, and many of them exhibit pronounced (above 300 S/cm) electron conductivity, even exceeding 1000 S/cm for Magneli phases (Ebonex). Furthermore, a majority of hypo-d−(f)-oxides and in particular of higher altervalent numbers feature a prevailingly high percentage of spontaneous dissociative water molecule adsorption[11,12] (eq 1-a) and, hence, the enhanced surface membrane type of hydroxyl ion migration mass transfer[13] (eq 1-b and 1-c), the latter being, as the

DOI: 10.1021/jp510234f
J. Phys. Chem. C 2015, 119, 11267−11285

XPS measurements show (discussed later), even some sort of common interfering effect, too

$$Nb_2O_5 + 5H_2O \Leftrightarrow 2Nb(OH)_5 \quad (1\text{-a})$$

$$Nb(OH)_5 + Pt \Rightarrow Nb(OH)_4^+ + Pt - OH + e^- \quad (1\text{-b})$$

$$Nb(OH)_4^+ + 2H_2O \Rightarrow Nb(OH)_5 + H_3O^+ \quad (1\text{-c})$$

$$\sum Pt + 2H_2O \Leftrightarrow Pt - OH + H_3O^+ + e^- \quad (1)$$

ending up with the prevailing electron transfer to the interactive supported metallic catalyst, so that the Pt−OH behaves as a pronounced dipole species[14] and, thus, exhibits strong spillover surface repulsion, transfer, and distribution. At the same time, the highly pronounced reversible potentiodynamic peaks testify for the extremely fast and independent overall spillover reaction (eq 1), in both directions,[2,3] primarily used for DL pseudocapacitance adsorptive charging and discharging and then being ready and available for fast heterogeneous electrocatalytic reactions. In the same context, it would be significant to infer that whenever anodic oxidation reactions of the Pt−OH (Au−OH) exceed, at least for an order of magnitude, the disproportionation rate (eq 2), such as the ones with HCHO[4−6] and other aldehydes, simple alcohols, and their acids, then these succeed to suppress and remarkably postpone the Pt═O growth all along the potential axis until the close proximity of oxygen evolving limits and, consequently, are an experimentally confirmed enormous broad extension growth of the Pt−OH (Au−OH) adsorption peak (Figure 2, a,b). In fact, since Pt−OH (Au−OH) as the reactants belong to (electro)catalytic heterogeneous surface reactions and are insoluble in aqueous media, to approach the effect similar to the one just inferred with HCHO and then partially suppress or completely eliminate the surface oxide adsorptive growth (eq 2), along with avoiding the corresponding reaction polarization, and create the reversible electrocatalysts for the ROE (ORR, OER) (eq 3), interactive hypo-d−(f)-oxide supports yielding the advanced continuous, recoverable, and renewable latent storage of primary oxides have been employed[4,5] and hence are always ready for the Pt−OH spillover and electrode reactions.

In such an overall constellation, individual hypo-d−(f)-oxides, and even more so their mixed valence composite compounds, when in the expanded (sol−gel synthesis with thorough liquid CO_2 supercritical drying) hydrated surface state (Figure 3), behave as unlimited latent storage and spillover sources of the primary oxide,[5,15,16] continuously being renewed and recovered simply by water vapor supply and instantaneously proceeding with spontaneous dissociative adsorption of water molecules and corresponding distribution of exposed hydrated hypo-d−(f)-oxides available for the membrane migration surface transfer (Scheme 1).

In such a respect, it is certainly worth mentioning the autocatalytic Ertel[17] effect of water molecules for the Pt−OH growth that mostly occurs in all heterogeneous (electro)catalytic oxidation processes, particularly when these water molecules appear as dipoles polarized within double layers (eq 1). Haruta[18] in the same sense has pointed out the lowest threshold moisture content below which there is no CO oxidation upon interactive supported catalysts (nanostructured Au/TiO_2). Meanwhile, Boudart[19,20] inferred on the continuous minimal monolayered water vapor condensation (Figure 3), as the precondition state for fast spillover of H-adatoms upon hydrated (Pt/$Nb(OH)_5$) and *vice versa* for Pt−OH,[2,3] even at ambient temperature, while in the dried oxide state, it needs be at 400 °C. In fact, an entirely

Scheme 1. Visual Presentation of Novel Spillover Latent Storage Pt−OH Interactive Supported Model Type Electrocatalyst for Oxygen Electrode Reactions, Shown for Pt/Nb_2O_5, TiO_2/$Nb(OH)_5$, and $Ti(OH)_4$

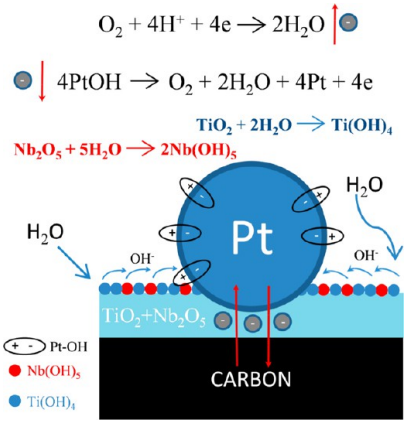

thermodynamic equilibrium is established (Pt/$H_xNb_2O_5$ ⇔ Pt/$Nb(OH)_5$), which enables the reversible alterpolar interchanges and therefrom the substantiation of superior revertible cells altering between PEMFCs and WE (water electrolysis), otherwise of substantial significance for the hydrogen energy balance and performances. In other words, no spillover of primary oxides (Pt−OH, Au−OH) substantially means that there are no reversible alterpolar changes and no advanced revertible cells!

The most fascinating results in heterogeneous catalysis were obtained by Haruta[18,25] long ago with nanostructured gold interactive supported upon anatase titania (Au/TiO_2). The same nanosized Au clusters, once plain and then hypo−hyper-d−d-interelectronic titania supporting bonded, mutually differ for several orders of magnitude in catalytic activity for the highly efficient quantitative reaction (trace amounts removed for human protection) with CO at the extremely low water content threshold level. The same catalyst metal (Au) differed only in the interactive hypo-d-oxide support in the presence and/or absence of anatase titania (101), while the catalytic activity has been distinctly, exponentially different and broadly proved. For catalytic science it was *a priori* clear that some superior reaction occurs initiated at and provided by the exposed titania surface. In other words, the latter is predestined to be ready and highly susceptible for spontaneous adsorptive dissociation of water molecules ($TiO_2 + 8H_2O \Rightarrow Ti(OH)_4 + 4H_3O^+$), otherwise being already revealed as the subject of latent storage and the Au−OH spillover,[5,30,33] decisive for both heterogeneous catalytic oxidation and reduction reactions[5,30−35,45]

$$Au + Ti(OH)_4 \Leftrightarrow Au-OH + Ti(OH)_3^+ + e^- \quad (1A)$$

(see XP spectra analysis below). The final and some similar and congenial relations have then been named *the equations of the latent storage and reversible spillover of the primary oxides* (Pt−OH, Au−OH).[5] Such an observation has been the initiative and intuitive idea to introduce and develop the interactive hypo-d−d−(f)-oxide supported catalysts in electrocatalysis.[5,30−35,45]

Interchangeable Interfering Reversible and Polarizable Oxygen Electrode Reactions. In general, the nanostructured Pt (Au) electrocatalyst selectively interactive grafted upon hypo-d−(f)-oxide supports, when the latter exist in the hydrated external surface and/or internal bulk matrix state (Scheme 1), exhibits enriched Pt−OH (Au−OH) latent storage,

DOI: 10.1021/jp510234f
J. Phys. Chem. C 2015, 119, 11267−11285

as the feedback oxophilicity effect and property. The corresponding primary oxide then continuously features renewable spillover, simply by water vapor supply (surface phenomena, no concentration polarization), and further continuously yields spontaneous dissociative adsorption of aqueous species, so that the reversible anodic oxygen evolution (eq 4) now takes place straight from the pronouncedly high and also the highly reversible Pt−OH (Au−OH) adsorptive peak capacities (Figures 3 and 4)[4,5,21]

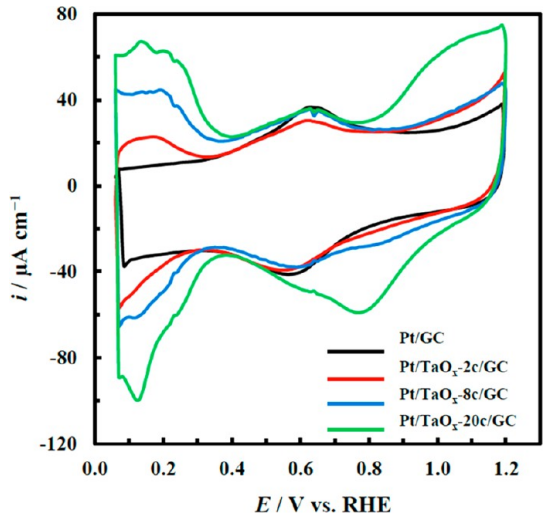

Figure 4. Cyclic voltammograms scanned at the Pt/GC and Pt/TaOx/GC catalytic electrodes with 2c, 8c, and 20c (cycles) in Ar-saturated 0.5 M H_2SO_4 solution at a scan rate of 50 $mV{\cdot}s^{-1}$, revealing the effect of proportional increasing of interactive Pt, supporting Ta_2O_5 deposit on the Pt−OH spillover effect and growth for the ORR (courtesy of T. Ohsaka; published with permission from RSC Publishing[15]).

$$4Pt{-}OH \Leftrightarrow O_2 + 2H_2O + 4Pt + 4e^- \quad (4)$$

and, hence, at the thermodynamic equilibrium (ROE) potential value. Quite on the contrary, in classical issues (Figure 1), the latter occurs from the strong irreversibly deposited and highly polarizable monolayer of the Pt═O (eq 2) and, while being deprived of primary oxides, at rather high anodic overpotential values

$$2Pt{=}O \Rightarrow O_2 + 2Pt + 4e^- \quad (5)$$

The same consequently alternately occurs in both these reversible and/or irreversible states, as concerns the ORR, all along the reverse cathodic scan and polarization (Figures 1, 3, and 4).[4,5,21] The transient between the reversible and irreversible status features some sharp thresholds as a function of both hypo-d−(f)-oxide unit content[15] and/or wetness percentage (Figures 3 and 4)[4,5] and substantially reflects the Pt−OH (Au−OH) properties (present or absent) for the oxygen electrode reactions. In such a context, plain and noninteractive supported Pt (Pt/C), in the absence of primary oxides and thereby established or *a priori* existing in the broad reaction polarization range, by no means can feature the overall reversible oxygen electrode properties within the whole potential axis, in between the hydrogen and oxygen evolving limits. Thus, there exists either the reversible behavior in the presence or continuous external supply of primary oxides or the highly irreversible properties in the absence of the latter (Pt−OH → 0, Au−OH → 0), and this is the substance for Pt and Au electrocatalytic properties!

In such a context, the simple stoichiometric combination of eq 1 and eq 4 reveals that the overall reversible anodic oxygen evolution initiates from water molecules (eq 1) and obeys the auto- or self-catalytic Ertel framework,[17] with the general oxidation mechanism based on and catalyzed by M−OH species or the primary oxides as the main interfering electrocatalytic species, and substantially takes place at the reversible oxygen potential value; the same is true in the reverse cathodic ORR scans. However, when oxygen evolving initiates from the Pt (Au) monolayer covered by the strongly adsorptive and polarizable surface oxide (Pt═O, Au═O), the anodic and reverse cathodic reaction both have to overcome remarkable overpotentials (eq 5, adjoined with eq 2). This is the substance and difference as concerns the irreversible plain (Pt, Au) and noninteractive supported Pt/C (Au/C) and/or the enriched latent storage and continuous external spillover feeding of the primary oxide for interactive hypo-d−(f)-oxide-supported Pt electrodes. The fascinating and incredible surprising facts, meanwhile, are that such simple distinct phenomena have been obscure and unknown in electrocatalysis for many decades until now.

Electrocatalytic Consequences. Since the Pt (Au) electrocatalyst becomes interactive d−d−(f)-bonded with and grafting fixed upon hypo-d−(f)-oxide type catalytic supports in a new composite nanostructure, there is no longer metallic nanoparticle surface diffusion and agglomeration nor any Nafion membrane crossover of hydrogen. Even more so, for the same reasons, the lifetime of Pt (Au) is at least two times longer and can be guaranteed. Alterpolar spillover changes in the revertible PEMFC versus WE proceed reversibly and instantaneously smoothly and enable their superior unique operation and interchanges. There is a lot of parametric and structural variability for the voltage/current optimization and stability, such as the hypo-d-oxide radius of small, medium, and large d−(f)-metals (Y, Ti, Nb, Ta, W, Ce, Gd, Ho, La, etc.), to keep the low Tafel slope within the operating range, 0.0−1.0 A cm^{-2}. Since some of the hypo-d−(f)-oxide supports of composite electrocatalysts (Nb_2O_5, Ta_2O_5, TiO_2) feature advanced electron conductivity, nanoparticulate carbon carriers and current collectors can be completely avoided which is substantially significant for WE and mostly for anodic oxygen evolution. In such a respect, the present paper defines the main substantial and advantageous frameworks in electrocatalysis of reversible electrocatalysts for oxygen electrode reactions (mostly ORR and AOE), primarily for L&MT PEMFCs, WE, and their revertible combinations, and the overall main conclusion hopefully represents the most important contribution since Sir William Grove. All stated herein for Pt is even more true for Au when oxygen electrode reactions are in consideration (ORR, OER).[21−26]

Mixed altervalent hypo-d−(f)-oxide supports, depending on their preceding thermal treatment, feature advanced electron conductivity from and even above 1000 $S{\cdot}cm^{-1}$, for Magneli phases, down to about 300 $S{\cdot}cm^{-1}$ for average composites and this way enable us to replace and even completely remove nanostructured carbon as a noninteractive catalyst support and current collector. However, except for the OER, when carbon becomes partially the subject of anodic oxidation, nanoparticulate carbon still satisfies requirements for its nominal purposes. In fact, the main benefit comes from the dissociative adsorption of water molecules upon mixed valence hypo-d−(f)-oxide supports, enabling us to increase the latent storage capacity, and therefrom the yielding Pt−OH (Au−OH) spillover intensity and/or the higher current density at the more reversible electrode potentials. In the same respect, the supercritical drying within the sol−gel procedure for hypo-d−(f)-oxide supports

DOI: 10.1021/jp510234f
J. Phys. Chem. C 2015, 119, 11267−11285

development and enables us to extend remarkably the available surface for dissociative water molecule adsorption and consequently enlarge the Pt−OH latent storage and spillover intensity.

The actual target: Tafel slopes of 60 mV/Dec or η = 180 mV at 1000 mA·cm^{-2} or ideally 30 mV/dec, or 90 mV at 1.0 A·cm^{-2}.

Hypo−Hyper-d−d-Interelectronic Bonding and Interfering Spillover Nature of Electrocatalysis for Hydrogen and Oxygen Electrode Reactions. Where does the link between the hypo−hyper-d−d-interelectronic bonding and interactive SMSI synergistic electrocatalytic effects lie in the broader interfering spillover sense? The whole electrocatalytic theory[9,27] relies on the Brewer[8] intermetallic bonding model and Friedel[28,29] hypo−hyper-d−d-electronic correlations. They both infer that the stronger the hypo−hyper-d−d-intermetallic cohesive bonding, the more strengthened, more stretched, and more exposed the d-orbitals are within the ideal symmetric intermetallic phases, like $ZrNi_3$, $HfPd_3$, $MoPt_3$, $LaNi_5$, $La_xCe_{(1-x)}Ni_5$, etc., and thereby the weaker and easier the cleavage of their adsorptive intermediates (Pt−H, Pt−OH) in the RDS and the higher the reaction rate and the yielding overall catalytic activity.[4,9,27−35] The same Brewer[8] type d−d-intermetallic bonding model has been much earlier anticipated and is the preceding basis for the Tauster[10,36,37] promotional SMSI effect, with the far-reaching consequences in both heterogeneous catalysis and electrocatalysis. The latter systematically predetermined interactive grafting[31−35] and the homogeneous, even uniform, distribution of individual and prevailing hyper-d-metallic catalysts upon hypo-d-oxide supports.[4−6,21,34,35] The same type of hypo−hyper-d−d-interactive bonding between nanostructured hyper-d-metal particles of such composite catalysts and their hypo-d-oxide supports additionally reinforces the entire electrocatalytic activity effect based on the overall interactive d−d-interelectronic bonding strength, similarly as cohesive energy itself defines and advances the electrocatalytic activity for nanostructured monophase systems.[4−6,21] In fact, the interactive hypo−hyper-d−d-interelectronic bonding strengths belong to the strongest bonding effectiveness in the whole chemical science[4,9,21,27] (Figure 9, ref 5), sometimes even proceeding so vigorously with an exceptionally intense explosion ($HfPd_3$)[8] that they result in extra high intermetallic phase stability[8,9] and consequently high electrocatalytic activity for the HER.[27] In the same context, one of the striking issues and contributions of the present paper is that every hypo−hyper-d−d-interelectronic bonding effectiveness exceeds the entering value of individual transition metal cohesive energy strength and in particular all hypo−hypo-d−d- and/or hyper−hyper-d−d-interelectronic bonds! The pronounced cathodic and anodic yielding of interactive spillover contributions within and based on the SMSI have been significant for the present theory and its embodiment in electrocatalysis of both hydrogen and oxygen electrode reactions, particularly for low and medium temperature (L&MT) PEMFCs and WE.[4,5,31−37] While in aqueous media, plain nanostructured Pt (Pt/C) features the catalytic surface properties of Pt−H and Pt═O, missing any effusion of other interacting species, and a new generation of composite interactive supported (SMSI) electrocatalysts in the condensed wet state primarily characterize extremely fast reversible spillover interplay of either H-adatoms or the primary oxides (Pt−OH, Au−OH), as the significant pronounced synergistic advanced interactive electrocatalytic ingredients.[4−6,31−35]

Volcano plots of various physical and chemical properties along transition series reveal, by their repeating symmetry of characteristic parabolic (volcano) curves, the periodicity features of elements,[29,38] based on the d−d-electronic correlations,[28] with similar symmetric shape, and, consequently, when plotted one into other, together yield various linear interdependences like cohesive and surface free energy.[38,39] In the same sense, the logarithm of exchange current density in electrode kinetics for the hydrogen electrode reactions (HERs) and/or work function values of transition elements obey the same typical volcano plot along the Periodic Table and together with the Fermi energy (and/or its wave vector) reflect the wave nature of electrocatalysis, while the resulting linear interdependence with cohesive or surface free energy brings all these interrelated functions and their properties to the common universal sense and meaning. In fact, all such volcano plots along the transition series substantially mean and reveal the common fundamental physical properties and their correlating interdependences, all substantially based upon the d-electronic density of states, d-electronic configuration, and structure of d-metals, their Fermi level, and their variations along transition series. As a consequence, the d-band of transition elements has been confirmed to play a crucial role in the bonding, adsorptive, catalytic, and electrocatalytic properties, and consequently, any search for advances and synergism among the latter should be based on the d−d-interelectronic correlations and modifications.[27,35,35] Such a state of theoretical knowledge and experimental evidence leads to the conclusion that every hypo−hyper-d−d-interelectronic phase diagram behaves as the part of the Periodic Table between the two initial periods of the interacting ingredients.[38−42] Their intermetallic phases in between and/or along the phase diagram are of the same average d-electronic configuration, replacing the missing elements in their energy state, level, and behavior and, consequently, have been used to assess the synergistically active electrocatalysts for the HER (Figure 1, ref 4). These theoretical and experimental facts can then be employed to predict the synergistically active electrocatalysts from the peak values of corresponding semivolcano plots along each hypo−hyper-d−d-interelectronic phase diagram[38,40] and further catalytically advance by the interactive hypo-d-oxide interfering spillover contribution,[4−6,30−35] displayed more systematically and more thoroughly in the present and preceding study.[5] Thus, one of the guiding aims should have to be to assess experimentally or theoretically and consequently correlate the actual hypo−hyper-d−d-interelectronic SMSI effect or hypo−hyper-d−d-interbonding effectiveness for a new type of interactive supported composite (Pt/Nb_2O_5, TiO_2/C, Pt/Ta_2O_5, TiO_2/C, or more complex composites for the HER, $HfPd_3/Nb_2O_5$,TiO_2/C) electrocatalysts. The formal difference is that interactive bonding is interatomic or intermetallic (Brewer−Friedel correlations), while in the more complex Tauster SMSI sense,[10,36,37] they are interionic−intermetallic interactions or all together hypo−hyper-d−d-interelectronic bonding correlations in electrocatalysis.

Stepwise Survey of the Theory Development and Experimental Evidence of Its Confirmation. Although Pt best satisfies electrocatalytic requirements of PEMFCs for hydrogen electrode reactions (HERs), along with many more common transition elements (Ni, Co), both common energy chart diagrams (Figure 5) and interconnected cyclic voltammograms (Figure 1) heuristically show that the reversible behavior for cathodic oxygen reduction (ORR), like a broad plateau in the energy conversion, starts within the potential range of the reversible peak of the Pt−OH desorption. Consequently then, overall losses within the preceding critical potential range of the

DOI: 10.1021/jp510234f
J. Phys. Chem. C 2015, 119, 11267−11285

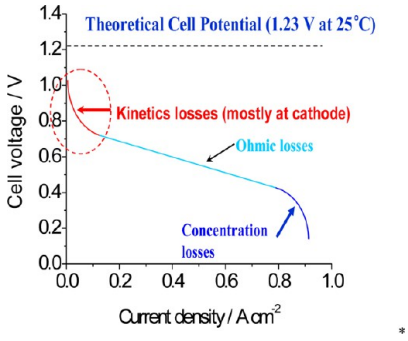

Figure 5. Classical and characteristic energy chart diagram for nanostructured Pt/C electrocatalyst in LT PEMFCs.

Pt═O reaction polarization (Pt−OH → 0; Pt═O → 1) amount to more than half of the thermodynamic available values, or about 600 $mV{\cdot}s^{-1}$. The main energy barrier obstacle arises as the imposed reaction polarization between the reversible adsorption/desorption peaks of the primary oxide growth and removal (eq 1) and anodic oxygen evolution, in both potential scan directions, as the result of irreversible disproportionation (eq 2) and transition of Pt−OH (Au−OH) into highly polarizable, remarkably irreversible, and strongly adsorptive surface oxide (Pt═O, Au═O). As the result, plain and noninteractive supported Pt (Au) electrocatalysts consequently then continuously lose their initial and nominal catalytic features along with the irreversible surface oxide coverage (Pt═O → 1, Au═O → 1) and thereby imposed strong reaction polarization. Thus, ever since Sir William Grove[1] invented gaseous type fuel cells (FCs), the electrocatalytic search for the reversible oxygen electrode (ROE) and, most particularly, the ORR became the main challenge and imperative impact target in electrochemistry of aqueous and PEM media, while its substantiation has been the leading and main motivating subject matter of the present paper. The substance is to replace the potential range of the strong reaction polarization of the monolayered surface oxide deposit (Figure 1 and 5) by the latent storage of the reversible spillover (electro)catalysis of their ideally equimolar concentration ratio (Pt−OH:Pt═O ≈ 1:1, eq 3) and make Pt (Au) catalytically reactivated within the polarizable range and all over the potential axis between hydrogen and oxygen evolving limits, back and forth. Otherwise the plain and noninteractive supported Pt (Au) is for a broad potential range substantially and highly polarizable electrode even when with extremely developed surfaces.

General Theory and Its Substantiation. Whereas hydrogen molecules undergo spontaneous adsorptive dissociation on plain Pt and noninteractive supported (Pt/C) and H-adatoms (Pt−H) establish thermodynamic equilibrium of the RHE (reversible hydrogen electrode, $(Pt(H_2)/Pt{-}H/H_3O^+)$), within the above identified critical reaction polarization range, Pt (Au) is deprived by the irreversible disproportionation reaction (eq 2) from the effectively available Pt−OH to provide reversible properties for the ROE ($(Pt(O_2)/Pt{-}OH, Pt{=}O)/OH^-$) and both together the reversible hydrogen fueled L&MT PEMFCs. In other words, the substantial and decisive point is that immediately after and even within the highly reversible peak of the anodic Pt−OH growth (eq 1) there proceeds the strongly adsorptive and highly polarizable electrode process of its irreversible Pt−OH → 0 (Au−OH → 0) disproportionation into the stable surface oxide (Pt═O → 1) (eq 2) and that its irrecoverable deprived status and absence imposes such a typical and critical reaction polarization range (Figures 1 and 5) all along until vigorous anodic oxygen evolution and equally so in the reverse scan direction.

In such a respect, polarization properties of some typical and characteristic novel interactive hypo-d−f-oxide supported nanostructured Pt electrocatalysts for both the ORR and OER[4,5,21] enable us to select some diagnostic kinetic criteria on the way toward the ROE, revealed from their Tafel plots: (i) nanodispersed Pt/C clusters (10 wt % Pt) noninteractive adhering upon sol−gel developed indifferent nanoparticulate E-tek, Inc., Vulcan-XC-72 carbon (240 sq.m/g) carrier and current collecting species, considered for the classical issue of such an electrocatalytic activity comparison; (ii) the interactive supported nanostructured Pt particles upon both the extra stable and electron conductive (300−1000 S/cm), ceramic Magneli phases (Ebonex), $Ti_nO_{(2n-1)}$, in average Ti_4O_7, usually defined as a shared rutile structure, accommodating the oxygen suboxide deficiency in the structure by the formation of crystal shared planes along the *n*th layerlike plane of octahedron, so that Ti_4O_7 has one TiO for every three TiO_2 layers; (iii) advanced interactive selective grafted and homogeneously distributed nanostructured Pt clusters down to the prevailing (2.2 ± 0.2 nm) nanosize, upon the optimized structure of mixed valence hypo-d-oxide compounds (Pt/Nb_2O_5,TiO_2/C), and even further extended (iv) composites with hypo-f-oxides (Pt/Nb_2O_5, CeO_2, TiO_2/C, including doped GdO_2, HoO_2, and/or LaO_2 itself) and their relative combinations of extra high stability and remarkable electron conductivity, too. Such comparable diagnostic Tafel polarization interdependences distinctly displays Figure 6,

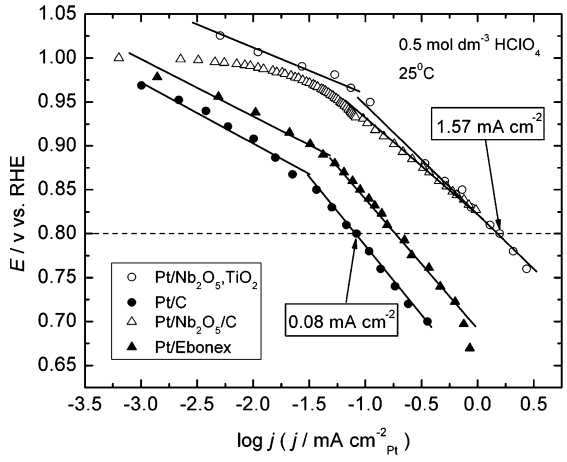

Figure 6. Tafel plots for the cathodic ORR scanned on RDE in 0.5 M $HClO_4$ solution at 25 °C for E-tek, Inc., Pt/C (Vulcan XP-72, closed circles); Pt/Ebonex (Magneli phases, closed triangles); Pt/Nb_2O_5 (20 wt %)/C (70 wt %) (open triangles); and Pt/Nb_2O_5 (5 mol %), TiO_2 (95 mol %) (open circles) (Pt 10 wt % in all instances).

with differences of more than an order of magnitude in the electrocatalytic activity for the ORR that arise ***only as*** the result of different hypo-d−f-oxide type of interactive catalyst supports, relative ratios of their amounts versus metallic part of the catalyst (Pt), and their corresponding SMSI.[10]

Leading Idea and Its Confirmations for the ROE Electrocatalysts. Some subtle potentiodynamic survey of fundamental significance has then been focused on the actual mixed interfering Pt−OH/Pt═O coverages at selected points within the characteristic potentials close to the open-circuit value and all along the reversible potential range of low Tafel line slopes (mostly 30 mV/dec, Figure 7). The main conclusions then

DOI: 10.1021/jp510234f
J. Phys. Chem. C 2015, 119, 11267−11285

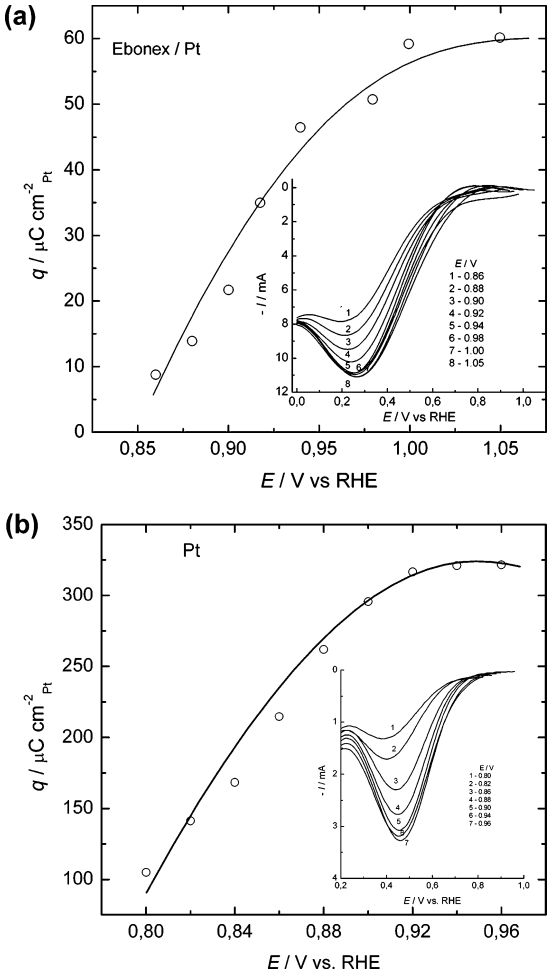

Figure 7. (a) Charge density (q) that required adsorbed oxygen species (Pt−OH/Pt═O) for their reduction, presented as a function of potential for the Pt/(Magneli phases) (5 mg) electrode; same as in Figure 6.[4,21] The inset shows potentiodynamic I vs E relations scanned from indicated different initial potentials (hold) with sweep rate of 5 V·s^{-1}. (b) Same as in (a) but for polycrystalline Pt metal.

have been that Pt electrodes, both plain and interactive supported upon hypo-d-oxides, have been covered by mixed (Pt−OH, Pt═O) oxides (besides many other experimental methods, *in situ* and *ex-situ* XPS confirmed[6]), while at higher irreversible polarization (120 mV/dec), they were completely deprived from such adsorptive layers.[21] In other words, while within the reversible range, the ORR is associated with and *proceeds upon mixed oxide covered Pt surface*, as the interfering self-catalytic spillover electrode process (eq 3), otherwise known as the fastest reaction step.[7] On the contrary and substantially different, the oxide-free Pt surface imposes much higher polarization for the direct electron transfer reaction to occur.[6,21] Thus, the conclusive observation has now been that *Pt oxides play the same self-catalytic role to establish the ROE properties* as the spontaneous hydrogen (Pt−H) adsorption does for the RHE. In fact, the leading idea consists now of the extension of the reversible Tafel plot for the ORR all along the potential axis down from or up to the thermodynamic value (1.29 V vs RHE). The latter implies enriched external latent Pt−OH storage and continuous spillover supply all along in both scan directions and particularly within the critical reaction polarization potential range (Figures 1 and 5). Namely, so far the problem and obstacle were the initial highly reactive polarizable potential range of strongly adsorbed monolayered Pt═O and the missing Pt−OH, which cannot be supplied from aqueous solution but only as the adsorptive surface species. These rather specific potentiodynamic measurements even more clearly show that the ORR upon the Pt/Ebonex Magnely phase starts and finishes at remarkably more positive potential values (1.05 down to 0.86 V, versus 0.95 down to 0.8 V, all versus the RHE, Figure 7), relative to polycrystalline Pt metal and/or nanostructured Pt/C.[4,21] Meanwhile, in addition, the other two congenial issues (iii) and (iv) initiate with 1.29 V as the completed reversible property of the ROE (Figures 3 and 4) and have been the ones of the main substantial conclusive remarks on the way toward the ROE (electro)catalysts. These, as the substantial impacts, afford and enable the reliable link between the reversible and polarized oxygen electrode properties. In fact, the just displayed analytical survey and experimental evidence belong to the crucial arguments that the interfering oxide ratio [Pt−OH]/[Pt═O] means the optimization key (eq 3), to approach the ROE and corresponding electrocatalytic effects enabled by the primary oxide latent storage and spillover.

In such a respect, the guiding concept implies homogeneous nanostructured distribution and selective grafting, while interactive hypo−hyper-d−d−(f)-interelectronic bonding of Pt (Au) nanoclusters upon various individual and preferably mixed valence hypo-d-oxide supports (Figure 7), taken for the reversible external interconnected latent storage and spillover Pt−OH (Au−OH) sources (Scheme 1), primarily Nb_2O_5, TiO_2 (or Ta_2O_5, TiO_2), because of their improved membrane type migration, much advanced both the stability and electronic conductivity. In such a constellation, nanoparticles of solid oxides and Pt establish the SMSIs, the strongest ones in all of chemistry (Figure 9, ref 4), together with the electron conductive transfer. Meanwhile, and in addition, the external surface (and even internal bulk) of the hypo-d-oxide deposit undergoes spontaneous dissociative adsorption of water molecules and thereby becomes, along with continuous further water vapor supply (Scheme 1), the renewable and dynamically almost unlimited latent storage and spillover source of the Pt−OH.

Spillover Phenomena in Electrocatalysis of the ORR. Spillover phenomena in general impose and imply strong dipolar repulsion forces, when RDS intermediates (Pt−OH, Pt−H) partially transfer their charge to the metallic catalyst surface and become dipoles.[14] The driving force for such effusion effects imposes the gradient of electrochemical potential, which implies chemical potential for heterogeneous catalytic processes. Namely, the fundamental Guldberg−Waage law of mass action predicts that the faster the spillover effect of the reacting intermediate species in the RDS, the faster the corresponding electrode and/or, in general, heterogeneous catalytic reaction becomes.

Adsorptive Dissociation of Water Molecules and Membrane Type Surface Migration. The first decisive step toward the rather fast spillover of widespread phenomena of Pt−OH is the result of confirmed evidence of strong first-principles thermodynamics (density functional calculations, DFC) by Vittadini et al.,[11] where water molecules undergo prevailing spontaneous dissociative adsorption on anatase and even rutile titania and more so on the higher altervalent capacity hypo-d−d−(f)-oxides[12] of tungsten, molybdenum, tantalum, niobium, and/or cerium, etc. (Figure 2, in ref 21), as the general oxophilicity properties of hypo-d-electron metals. In addition, the first-principles molecular dynamics simulations showed the existence of a mechanism for thermodynamically favored

DOI: 10.1021/jp510234f
J. Phys. Chem. C 2015, 119, 11267−11285

spontaneous dissociation of water molecules even at low coverage of oxygen vacancies of the anatase (101) surface[12] and, consequently, at the Magneli phases, as a substantial suboxide structure significant both as a highly bulk electronic conductive, membrane type surface transferring hydroxide species and a superior interactive catalyst support. In fact, this is the status of reversible open-circuit dissociative adsorption of water molecules at the equilibrium or steady state, something like capillary phenomena in adsorption after some critical coverage extends. Meanwhile, in the presence of the nanosized metallic part of the catalyst, and continuous enough moisture supply, the directional electric field (or electrode polarization) further disturbs such an established equilibrium and dynamically imposes further continuous forced dissociation of water molecules and, as a consequence, their membrane transport properties (Livage et al.[13]) (eqs 1-a, 1-b, and 1-c summation ($\sum$) yields eq 1), definitely resulting with spillover features.

Such an oxide network, in particular of polyvalent (high altervalent numbers) hypo-d−(f)-elements, when in the pronounced hydrous state, distinctly behaves as an ion exchange membrane even for the surface hydroxide migration.[13] The latter sometimes appears even promoted by some intermolecular forces within mixed valence hypo-d−d-oxide supports (typical anatase TiO_2 versus Nb_2O_5 and/or Ta_2O_5, see further the study by XP spectra). This is one of the main distinct and striking points in the present theory. In fact, gels (aero and xerogels) are biphasic systems in which solvent molecules are trapped inside an oxide network, and such a material can be considered as water−oxide membrane composites.[13] At the same time, the highly pronounced reversible potentiodynamic peaks testify for the extremely fast and independent overall spillover reaction (eq 1), in both directions,[2,3] primarily used for DL charging and discharging pseudocapacitance[4,21] and always available for heterogeneous electrode reactions (see further details below).

Electrocatalytic Spillover Phenomena. Spillover effects and contributions in electrocatalysis were for a long time omitted and delayed, and though advantageous and superior for the additional driving force of electrode polarization, and the resulting migration of specific ionic and dipole species, the first knowledge and experience of electrochemical science is due to heterogeneous catalysis. The first spillover phenomenon in heterogeneous catalysis was observed and defined by Boudart[19,20] for the interactive supported bronze type (Pt/WO_3) catalyst, initially at high temperature (above 400 °C) for pure solid oxide system. Meanwhile, after the prevailing dissociative adsorption of water molecules on hypo-d-oxide supports of Pt, the fast interactive effusion of H-adatoms over its hydrated ($W(OH)_6$) surface becomes dramatically sped up even at ambient conditions in the ultimate presence of condensed at least monolayer aqueous precipitate, and *vice versa*, establishing capillary phenomena of speeding up effusion of the main catalytic reaction intermediates (Pt−OH). Such a striking sharp wetness impact upon the overall spillover phenomena associated with hydrated hypo-d-oxides in aqueous media implies an Ertel[17] autocatalytic molecular water effect as well, otherwise not well known in electrochemistry and electrocatalysis, which states that the catalytic reaction of hydrogen oxidation upon the Pt surface, even at deep low temperatures (140 K), proceeds with remarkable amounts of Pt−OH, as the decisive and accumulated intermediate, including the self-catalytic step with adsorbed water molecules (equivalent to but being faster in the electrochemical issues displayed by eq 1)

$$2Pt + O_{ads} + H_2O_{ads} \Rightarrow 2Pt{-}OH \quad (6)$$

In fact, Ertel has pointed out the substantial overall significance of water molecules in heterogeneous catalysis for oxidation processes that in general proceed over the Pt−OH generation and spillover and substantially imply the fundamental peak relations (eq 1) in the same way in (electro)catalysis. Meanwhile, since the slowest intermediate defines and describes the overall reaction for hydrogen and any other oxidation process, the primary oxide is the missing intermediate in the slower steps of the entire reaction mechanism, otherwise unavoidably based on and including the latter.

Such a Boudart spillover effect is significant for the evidence of the extremely fast widespreading spillover and thereby results in imposing the reversible hydrated substrate reduction.[19,20] The latter finally leads to the corresponding form of electrocatalytically active bronze ($Pt/H_{0.35}WO_3$) for cathodic processes, in which nonstoichiometric incorporated hydrogen obeys the same free reactive properties like adsorptive (Pt−H) and is the main source for the electrode or heterogeneous catalytic reactions. In other words, the point is that spontaneous dissociative adsorption of water molecules[11,12] imposes much smaller activation energy for transformation of the resulting hydrated $W(OH)_6$, into the corresponding bronze state, and occurs even *at ambient temperature* at a remarkable reaction rate. The latter then behaves remarkably different from the initial solid oxide WO_3 and, thereby, dramatically facilitates the overall spillover effect under pronounced wet status (the activation energies hence being in the ratio of 2.2, one with another). The alterpolar interchanges between the bronze type electrocatalyst and its hydrated state are correspondingly proved to occur instantaneously and reversibly fast, exactly because of the substantially facilitated Boudart[19,20] spillover effect, and behave as a thermodynamic equilibrium ($Pt/H_{0.35}WO_3 \Leftrightarrow Pt/W(OH)_6$ or $Pt/H_xNbO_5 \Leftrightarrow Pt/Nb(OH)_5$). In other words, such state-of-the-art properties enable us to perform (electro)catalytic processes from very high temperature down at ambient conditions, simply by the wetness effect.[4−6,21]

Hypo-d-electronic transition metal oxides usually feature several altervalent states even giving rise to interactive mixed valence compounds, such as, for example, TiO_2/WO_3, TiO_2/Nb_2O_5, TiO_2/Ta_2O_5, or $TiO_2/Nb_2O_5/CeO_2$, and then correspondingly increase the overall latent storage and spillover effect of both H-adatoms and primary oxides (M−OH). The whole spillover and SMSI effects behave as typical synergistic electrocatalytic properties, and no individual hypo-d-oxide enables as much as mixed altervalent composites. Such coinciding and interconnected events and phenomena have finally been perfectly and broadly tuned in a mutual phase, almost like a lucky concatenation, and enabled us to approach and substantiate the reversible electrocatalysts for the oxygen electrode reactions.

The problem so far was the unattainable nanostructured Pt-bronze, the catalytic activity of which exponentially increases with a decreased Pt nanosize approaching maximum at monatomic dispersion.[22] This requirement has now been fulfilled by the grafting implementation of Pt-acetylacetonate (Pt-acac) and the whole broad family of such rather extra pure, extra active, and mostly inexpensive initial acac ingredients, within colloidal particles of peroxopolytungstic acid, niobia (Nb_2O_5), tantalia (Ta_2O_5), and ceria (CeO_2) (Figure 8).[5] Such a homogeneous and even distribution of nanostructured Pt

DOI: 10.1021/jp510234f
J. Phys. Chem. C 2015, 119, 11267−11285

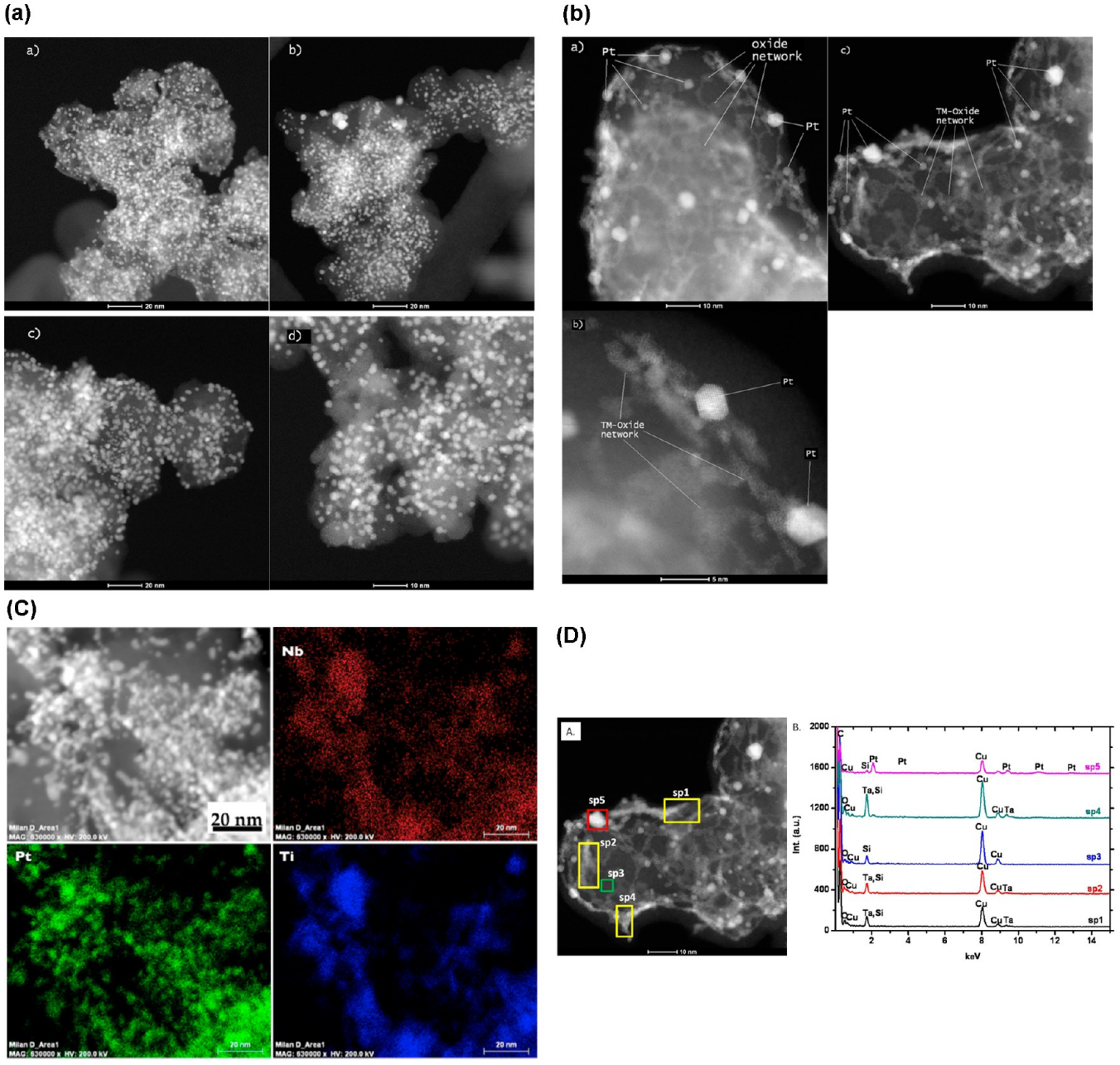

Figure 8. (A) Scanning transmission electron microscopy images in high-angle annular dark-field mode (HAADF-STEM) of TM hypo-d-oxide/carbon support material and nanostructured Pt electrocatalyst nanoparticles. (a) Composite simple basic Nb-oxide interactive (SMSI) supported electrocatalyst, {Pt (10 wt %)/20 wt % Nb_2O_5/C}; (b) Congenial mixed altervalent supported electrocatalyst, {Pt (10 wt %)/20 wt % Nb_2O_5,TiO_2/C}; (c) Composite interactive (SMSI) altervalent supported electrocatalyst of the same hypo-d-oxide structure as in (b) but of triple higher Pt weight percentage {Pt (30 wt %)/20 wt % Nb_2O_5,TiO_2/C}; and (d) Congenial altervalent supported electrocatalyst based on mixed W-oxide and anatase titania interactive supported Pt clusters. (B) Atomic-resolved HAADF STEM images analysis taken in different areas of the sample. Pt catalyst particles and transition metal Ta-oxide network are identified by labels and pointed out by relevant lines in images. (a) High-resolution HAADF STEM general view of the carbon support, Pt, and the Ta-oxide network; (b) detailed view of the Pt and Ta-oxide network showing the single Ta atoms of the oxide network (the oxygen atoms are not visible in this imaging condition), (c) overview of intricate Ta-Ox network on carbon support and strong interaction between the Pt catalysts only located on (or surrounded by) the Ta-oxide. (C) EDX spectra (or high-resolution energy-dispersive X-ray spectral) analysis of the elemental mapping that further reveals the overall elemental structure and distribution within the interactive hypo-d-oxide supported electrocatalyst, giving evidence that the Pt nanoparticles are only distributed on the oxide network and avoiding (no d−d-interaction) any carbon support. Elemental analysis over {Pt (10 wt %)/20 wt % Nb_2O_5,TiO_2/C}: (a) STEM image of the sample and elemental maps of (b) Nb, (c) Pt, and (d) Ti. (D) (a) STEM HAADF image obtained from the sample containing Pt(10%) -based catalysts on Ta_2O_5/C, corresponding nano-located areas for EDX survey and acquisition are highlighted as sp1 to sp5; and (b): EDX spectra generated from various nano-locations of the sample as highlighted in (a), presenting the variation of the chemical compositions within the same interactive supported Pt/Ta_2O_5/C sample.

particles, and such SMSI bonding effectiveness, so far was missing experimental evidence in PEMFC development.

One of the substantial and most serious problems associated with and accompanied by the time function of catalytic activity in both heterogeneous catalysis and electrocatalysis represents the impurity effect. Meanwhile, the interactive hypo-d−d−(f)-oxide (or better their mixed valence hypo-d−d−(f)-oxide compounds) supported hyper- (Pt, Au, Ru) and prevailing

DOI: 10.1021/jp510234f
J. Phys. Chem. C 2015, 119, 11267−11285

hyper-d-intermetallic phase type electrocatalysts ($MoPt_3$, $HfPd_3$) because the latent storage and continuous spillover supply of the primary oxide are effectively prevented and deprived from the impurity effect most particularly in the L&MT PEMFCs. While plain (Pt, Au, Ru) and noninteractive supported (Pt/C, Au/C) electrocatalysts in PEMFCs usually suffer from nanoparticle surface diffusion and agglomeration, increasing the effective current density and corresponding polarization, the interactive hypo-d−d−(f)-oxide supported ones never face such an essentially serious problem because of the extra strong (SMSI) interbonding effectiveness and thereby fixed nanostructured cluster positions. Such strong interactive grafted bonding and fixed homogeneous and even nanostructured distribution and position of metallic catalyst nanoparticles distinctly contribute to the remarkable extended, at least doubled, lifetime of composite multifunctional (at least bifunctional) Pt (Au) electrocatalysts. Finally, the overall electrocatalyst hypo-d−d−(f)-network effectively prevents the Nafion membrane crossover effect and eliminates such inefficiencies and dangers. Such the accompanying secondary effect contributions of interactive hypo-d−d−(f)-oxide and, even more so, mixed valence hypo-d−d−(f)-oxide supports, all together almost approach the overall primary electrocatalytic achievements and dramatically advance the entire value and significance of the latter.

UHRTEM Nanoimages and EDXS Elemental Mapping of Hypo-d-oxide Electrocatalysts. UHRTEM and in particular STEM imaging in HAADF mode with aberration correction (FEI Titan 80-300), equipped with a Gatan Imaging Filter (GIF) for energy-filtered imaging and an energy-dispersive X-ray detector for elemental analysis and mappings, reveal grafted Pt nanoclusters on hybrid hypo-d-oxides supports, with a rather uniform and evenly homogeneous distribution on average of about 2−2.4 nm in size on the best issues {Pt (10 wt %)/20 wt % Nb_2O_5, TiO_2/C}, (b), {Pt (10 wt %)/20 wt % Nb_2O_5/C}, (a), and {Pt (10 wt %)/20 wt % WO_3,TiO_2/C}, (d), obtained so far and in excellent agreement with size measurement by XRD.[5] Even more so, with three times larger Pt amount {Pt (30 wt %)/20 wt % Nb_2O_5,TiO_2/C}, (c), the homogeneous nanostructured Pt distribution keeps the same trend and in particular the average nanosize. Such a homogeneous, unusually narrow nanosize level of distribution has never so far been achieved (the interactive grafting SMSI effect) and confirms the reliable basis for the rather pronounced spillover effect and the unique electrocatalytic achievements. As the effect of selective interactive grafting of nanostructured hyper-d-Pt metal upon hypo-d-oxide supports, no single Pt cluster has been noticed on the prevailing carbon nanoparticle percentage of their otherwise highly developed exposed surface area, and no surface diffusion and no agglomeration exist either. It would certainly be worthwhile to notice a rather all over homogeneous widespread instance of the interactive hybrid hypo-d-oxide support structure and well distinct inter-d−d-bonded and interactive (SMSI) grafted fine Pt nanosized cluster upon them, as a unique nanostructured Pt-bronze substantiation of advanced electrocatalytic properties, primarily and mostly extended by the pronounced interfering Pt−OH spillover effect for the cathodic ORR.

Namely, atomic-resolved HAADF-STEM along with elemental mapping by energy-dispersive X-ray spectrometry (EDXS) observations strongly support the interacting (SMSI) and interfering spillover theory. The selective interactive hypo−hyper-d−d-interelectronic grafting distribution between Pt and Ta_2O_5 or Nb_2O_5 on the carbon support results in the interdependent Ta (Nb) oxide network structure, symmetrically surrounding the Pt cluster (Figure 8). High-resolution HAADF images obtained with aberration correctors of the electron probe (0.07 nm resolution) even resolve the individual Ta (Nb) atoms of the oxide network support (Figure 8, B&C). This structure of Pt surrounded by the Ta oxide network should then further result, right at the interface Pt/Ta_2O_5, as the nucleation center, and by the reinforcement of the overall SMSI effect at such a site, possibly as the $TaPt_3$ intermetallic phase, initially predicted by Tauster[10] and already XPS confirmed for $TiPt_3$ (Figure 3, ref 21), and provide the highest electrocatalytic activity as the result (cf. Figure 6).

Following the Pt loading on complex support (10 wt % Pt/20 wt % Nb_2O_5/C), HAADF, bright-field imaging, and elemental mapping (EDXS) demonstrate that crystalline Pt catalyst nanostructured clusters are homogeneously dispersed on the hybrid mixed valence hypo-d−d-oxide support (Figure 8, C). Combining imaging and elemental analysis, it was found that the catalyst nanoparticles are embedded into (and/or properly symmetrically surrounded by) the oxide layer as pointed out using white arrows in Figure 8, B. Higher loading on the same support, (30 wt % Pt/20 wt % Nb_2O_5/C) provides evidence of maintaining the same preceding uniform dispersion just within the optimal Pt/hypo-d−d-oxide support ratio (Figure 8, A). On the basis of elemental mapping with energy-dispersive X-ray spectrometry, it was enabled to deduce that the Pt nanoparticle distribution is strongly correlated with the location of the transition metal oxide and rather avoiding any carbon (no d−d-interactive bonding). When present, the thickness of the disordered oxide network varies between 1 and 2 nm.

Anodic HCHO Oxidation and Primary Oxide Spillover. Since the heterogeneous reaction of formaldehyde oxidation with Pt−OH, and in particular Au−OH, proceeds as a fast reversible mass transfer limited anodic process and since HCHO is soluble in all ratios in aqueous media, the primary oxide generation rate and its yielding spillover have primarily been investigated by potentiodynamic spectra within the broader concentration range and between hydrogen and oxygen potential evolving limits (Figure 2, a&b). More than an order faster anodic reaction is able to postpone within unusually long potential range the recombination of the primary (Pt−OH), into the more polarizable, stronger adsorptive, more irreversible, and more stable surface oxide (Pt═O) (eq 2). Formaldehyde oxidation starts at its reversible potential (0.32 V vs RHE), merges with the second UPD desorption peak of H-adatoms, and extends as an exaggerated broad twin peak all along the anodic scan, nearly until the beginning of OER (Figure 2a). In the same sense anodic Pt−OH striping CO oxidation on composite hypo-d-oxides supported Pt or Pt, Ru catalysts takes place even within the usual interval of UPD H-adatom desorption (Figure 7, ref 21) and dramatically exceeds the composite intermetallic Ru, Pt (or Ru−OH/Pt transferring and reaction effect). In other words, Pt−OH is available for reaction not only within its nominal reversible adsorption/desorption peak limits in regular mineral acid or alkaline aqueous solutions but also depending on the reactant (HCHO, HCOOH, CO, etc.) concentration, affinity, and its actual reaction rate, along an unusually broad and striking extendable potential range. Meanwhile, as the link of DL charging/discharging pseudocapacitance, it actually extends and appears available all along the whole potential axis of cyclic voltammograms. Such an unusually broader charge capacity area (Figure 2, a&b) usually features all the properties of typical under- and overpotential oxidation (UPO, OPO) peaks, in particular when compared with cathodic UPD properties of H-adatoms on Pt, Au, and various other transition metals. Such specific cyclic voltammograms clearly reveal the interference

DOI: 10.1021/jp510234f
J. Phys. Chem. C 2015, 119, 11267−11285

between Pt−OH and Pt═O and testify for the reaction polarization of the latter disproportionation (eq 2), along the distinctly and striking broader potential range. Such a potentiodynamic interplay between the primary (Pt−OH) and surface (Pt═O) oxides in the presence of and enabled by the heterogeneous catalytic HCHO reaction is of remarkable theoretical significance in the present study, when dealing with substantiation and optimization of composite electrocatalysts for the OER (ORR and OER).

Stepwise extension of positive potential limits toward the oxygen evolution reaction (OER) clearly shows (Figure 2, a&b) the absence and/or distinctly reduced Pt═O growth almost until oxygen starts evolving. Hence, during the reverse potential scan toward the HER, as the result of the latter, there arises and finishes the Pt═O desorption much earlier and of dramatically reduced charge capacity than nominally in the simple (the absence of HCHO), acidic, or alkaline solutions. As a result, the appearance of a characteristic sharp backward growing anodic current jump in the reverse potential sweep direction then testifies for the hysteretic (cathodic sweep, anodic peak) aldehyde oxidation within the former DL charging/discharging range and this way reflects the specific and highly reactive properties of the Pt−OH. In other words, as a corollary, there is no anodic aldehyde, alcohol, their simple acids, and even CO oxidation, nor the ORR, upon any M═O (Pt═O, Au═O) covered metal surface prior to the potential of molecular oxygen evolution, when the latter becomes broken, but only upon prevailing Pt−OH spillover deposits.

Namely, since aldehydes are often soluble in aqueous media almost in all ratios, their voltammograms at high contents feature imprinted extremely high both charge capacities and limiting currents at their peaks (Figure 2b) and thereby testify for almost unlimited reversible reaction rates (eq 1), as long as diffusional mass-transfer supply provides enough reacting species. This is even more so for interactive supported Pt and Au upon higher altervalent hypo-d-oxides and their mixed valence compounds, since these behave as highly enriched latent storage capacities of primary oxide spillover sources,[15,16,43,44] and when compared with the CO removal from the active electrode surface of Pt (Au).

This is the cause and reason why within the reversible part of Tafel plots the electrocatalytic metal (Pt, Au) surface is always covered by the interacting Pt−OH/Pt═O species and naturally tends to impose the reversible oxygen electrode properties, and these are the experimental evidence that the optimal catalytic rate implies their optimal ratio.

In such a context, meanwhile, one of the most outstanding observations has been that cyclic voltammograms of both formaldehyde (Figure 3, ref 43) and formic (muriatic) acid (Figure 4, ref 44) anodic oxidation distinctly differ upon plain (Pt) or noninteractive carbon-supported platinum (Pt/C), and the same, but more or less enriched and more exposed, support surfaces for the electrochemical reaction take place in specific amounts of interactive hypo-d- (Pt/Ta_2O_5/C,[43] and/or hypo-f-Pt/CeO_2/C[44]) oxides per available metal electrode surface. In other words, all the parameters and conditions being kept the same, the reaction rate becomes dramatically different upon various supported electrocatalysts in their hypo-d−(f)-oxide amounts and/or exposure, as the result of distinctly different additional Pt−OH spillover feeding and spreading effects and as the only distinctly imposed difference. Such a conclusive observation belongs to the main experimental arguments to prove the theory of the M−OH interfering self-catalytic spillover contributions in electrocatalysis of aqueous media (eq 3),[4,5,21] finally providing the ROE behavior and properties and tracing the way and entire approach for its substantiation. In such a respect, cyclic voltammograms more deeply enlightened and more revealed the spillover reaction impact properties of the Pt−OH.

Potentiodynamic Scans of Primary Oxide Latent Storage and Electrocatalytic Spillover Spreading. Some intermolecular compatible hypo-d-oxide mixed valence architectures (Pt/WO_3,TiO_2/C; Pt/Nb_2O_5,TiO_2/C), as the interactive catalytic submonolayer supports of high altervalent number or capacity, have been investigated by potentiodynamic scans to reveal both the primary oxide latent storage and resulting spillover yielding properties, along with same for H-adatoms. In this respect, cyclic voltammograms scanned at low moisture content of the He stream (just enough to enable basic electrode processes to occur and proceed), insufficient for WO_3 (or Nb_2O_5 and/or TiO_2) hydration, repeatedly reveal similar potentiodynamic spectra characteristic for indifferent carbon supported (Pt/C) or plain Pt itself (Figure 3), but with high double-layer charging capacity, because of the accompanying parallel charging of Vulcan carbon particles beside the metal (with correspondingly large charge value, Q_{DL} = 1.07 C).

In contrast to such fairly common occurrences, a continuous supply of saturated water vapor in the He stream at higher temperature (80 °C), imposing condensation (Boudart spillover precondition[19,20]) and leading to the appearance of wet titania−tungstenia mixed valence oxide composite (Scheme 2), along with spontaneous dissociative adsorption of water molecules all over its exposed surface,[11] as the interactive catalytic support, has been accompanied by the unusual phenomenon of a dramatic expansion of two reversible pairs of peaks of both the primary oxide ($Q_{Pt-OH(a)}$ = $Q_{Pt-OH(c)}$ = 1.453 C) and H-adatoms (247 versus 47 mC cm^{-2}, or in the ratio of about 5.3:1), chemisorptive deposition, and desorption (Figure 3), like a DC capacitance of an extremely developed electrode surface. Since these are highly reversible and evidently behave as the pronounced latent Pt−OH storage (cf. [4, 5, 11]), they keep their same extents even after multiple and repeating numbers of cycles at any other time. The latter have both been of unusually high spillover charge and discharge capacity values and for Pt−OH (UPD and OPD) shifted toward both much more negative and far positive potential limits, in common with Figure 2 a&b and the discussion thereon. In fact, two distinctly different cyclic voltammogram shapes and charge capacities (Figure 3) appear only as the result of the difference in water vapor supply, all other parameters being unaltered, and as the effect of the equivalent dipole (Pt−OH) charging and discharging of the double layer, since nothing else takes place in between. Every cessation in the steam supply instantaneously imposes the sudden reversible shrinkage of such rather exaggerated pairs of peaks down to the same initial potentiodynamic shape similar to the nanostructured Pt/C voltammogram spectra themselves. *Vice versa*, the renewed saturated water vapor feeding immediately leads to their former Pt−OH peaks and the same former charge capacities, namely, the effect later already noticed and scanned for formaldehyde[44] and formic acid[45] oxidation. Such an appearance without exception behaves as a typical reversible transient phenomenon by its endless altering repetition[4,5,21] and never appears upon the plain Pt/C electrocatalyst, both wet and/or dry, nor with small and insufficient amounts of catalytic hypo-d-oxide supports (Figure 4[15]).

DOI: 10.1021/jp510234f
J. Phys. Chem. C 2015, 119, 11267−11285

Scheme 2. Model Presentation of Electrochromic Individual WO_3 Layers and Composite Combinations of Tungstenia and Titania with Corner and Age Sharing Crystal Units within the Consistent Mixed Valence Compounds, SEM and TEM Confirmed for Amorphous Overall Structure: (a & b) As-Deposited Films, (c & d) As-Colored, and (e & f) As-Bleached Hypo-d-oxides[47,48]

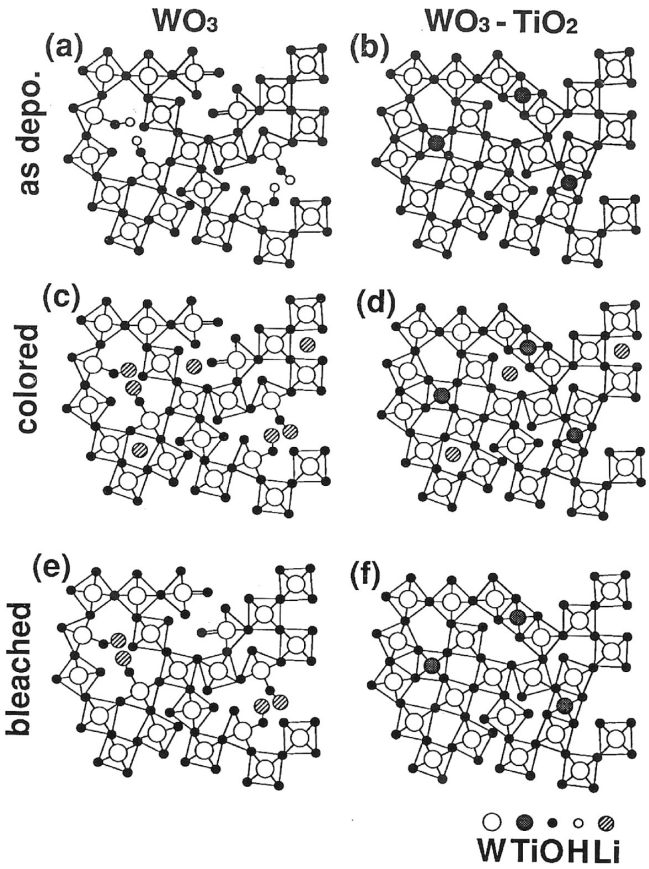

The complementary interactive Ta_2O_5-based electrocatalytic support strongly reinforces the just displayed potentiodynamic features of Pt/WO_3, TiO_2/C by their coinciding and congenial spectral behavior of their cyclic voltammograms: the distinct parallel growth of Pt−OH and H-adatoms adsorption and desorption peaks, reflecting their different accumulated latent charge capacities, as a function of the amount (charge density) of interactive composite hypo-d-oxide deposits per unit of exposed electrode surface (Figure 4).[15] In such a respect, for example, as the effect of a much smaller d-ionic radius, Y_2O_3 much more does so than Nb_2O_5 or WO_3. In fact, such Pt−OH latent storage growth (including the corresponding spillover effect) does not extend endlessly and usually passes over a remarkably pronounced maximum in the ORR catalytic rate and activity (see Figure 11, ref 9).

What is now the substantial difference between voltammograms in Figure 3, wet state, and Figure 2, a&b (or Figure 4)? Even when mostly suppressed in the surface oxide (Pt═O) adsorptive growth (Figure 2, a&b), the reversal backward cathodic scans on plain Pt proceed still highly polarized for about 600 mV with negligible or zero current, exactly corresponding to Figure 1. In other words, there is still no stored Pt−OH on plain Pt to start the self-catalytic interfering reaction (eq 3) of the ORR or HCHO oxidation. However, on the hypo-d-oxide interactive supported Pt catalyst, the *a priori* latently accumulated initial storage of the primary oxide from the beginning is ready and available and thence continuously provides, and spillover enhances the latter to proceed as the uninterrupted and extra fast reversible electrode reaction, as long as there is continuous water vapor supply. However, for the plain Pt (or Pt/C), the sudden hysteretic sharp anodic current jump in the course of reversal cathodic sweep (Figure 2, a&b) rearises at and coincides with the classical position of the reversible peak for the Pt−OH growth, reflecting the local interfering self-catalytic effects at such potential range, provided by the repeated Pt−OH spillover growth (Scheme 1). This is the striking point and the core substance of the present study, while Figure 3, supported by Figure 4, are the best illustrative issues of the substantiated reversible electrocatalyst for the oxygen electrode reactions (ORR, OER) (eqs 3 and 4).

What is substantially different now and of unique difference, when compared with any other simple or congenial cyclic voltammograms? The main decisive property is that currents continuously keep their increased constant level values and/or smoothly change ahead from them while cycling and when there appear certain growing adsorptive characteristics and in the course of the reversal potential scan, corresponding desorption peaks, all along the entire potentiodynamic cycles, being dependent only on the actual constant water wetness value.[33]

XPS Evidence for Membrane Type Surface Ionic Migration Providing and Yielding Primary Oxide Spillover. For the overall electrocatalytic view, while dealing with the ROE (ORR, OER), some common XP spectra of the composite interactive hypo-d-oxide TiO_2−Nb_2O_5 structure reveal some specific relations decisive for membrane type surface and bulk migration of hydroxide ions. In such a respect, Figure 9 displays comparatively presented the deconvoluted Ti 2p spectra of TiO_2−Nb_2O_5 and TiO_2 itself for interactive supported Pt catalysts. The main doublet in both XP spectra, at binding energy (Ti $2p_{3/2}$) 458.8 eV, is attributed to Ti^{4+} species.[46−48] In the case of the TiO_2−Nb_2O_5 mixed valence hypo-d-oxide support, a second doublet at binding energy (Ti $2p_{3/2}$) 455 eV is attributed to the contribution of Ti atoms in the Ti^{3+} state. Ti atoms in the other mixed hypo-d-oxide support TiO_2−WO_3 are detected only in the Ti^{4+} state.[49−53] Such an effect might be the cause for the higher synergistic electrocatalytic activity of the interactive Nb_2O_5 and similarly Ta_2O_5, mixed valence compounds with anatase (101) titania (TiO_2), relative to other hypo-d−d-oxide composites.[52−54]

In Figure 10 the deconvoluted Nb 3d XPS core-level spectra of TiO_2−Nb_2O_5 and Nb_2O_5 supported Pt catalysts are presented along with the former. In both cases only one doublet is apparent at binding energy (Nb $3d_{5/2}$) 207.1 eV that is characteristic for the Nb^{5+} state, which, when inserted into a titanium dioxide network, usually causes the effect in charge compensation.[49−54] The addition of such a charge can be compensated either by creating one vacancy of Ti per four introduced Nb ions or by the reduction of Ti^{4+} to Ti^{3+} per each inserted Nb^{5+} ion. Both of these effects can occur, with the latter being much more probable at relatively lower temperatures.[49,52,53] Quantitative analysis of the present results, using the Ti 2p and Nb 3d peak intensities (areas) corrected by the atomic sensitivity factors,[51−53] shows that the appearance of each Ti^{3+} corresponds indeed to the introduced Nb^{5+} ion.[52,55] In fact, EELS (electron energy loss spectroscopy) scans, in addition, clearly point to the valence variations of the oxide support, especially at the Ti edges[47,48] (cf. [56−58]).

DOI: 10.1021/jp510234f
J. Phys. Chem. C 2015, 119, 11267−11285

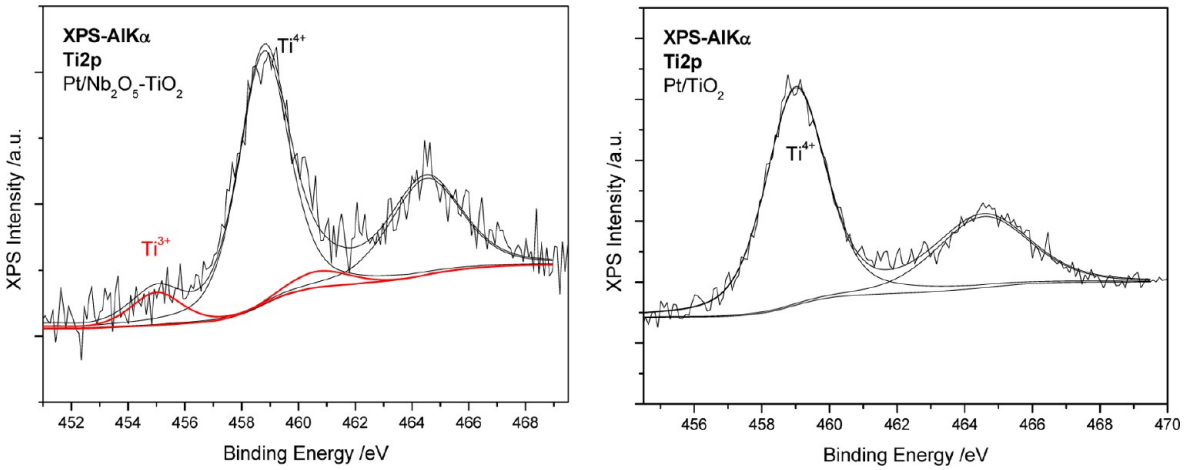

Figure 9. Deconvoluted Ti 2p XPS core level spectra of TiO_2−Nb_2O_5 (left) and TiO_2 (right) supported Pt catalysts.[6,45]

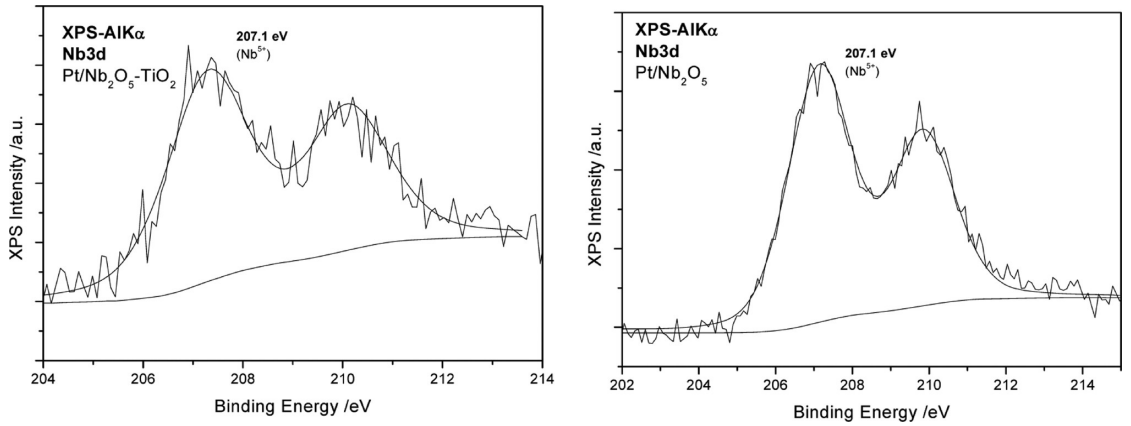

Figure 10. Deconvoluted Nb 3d XPS core-level spectra of TiO_2−Nb_2O_5 (left) and TiO_2 (right) supported Pt catalysts.[6,45]

There now arises a very interesting situation concerning the most promising electrocatalytic interactive hypo-d-Nb-oxide (and Ta_2O_5) structure, which at relatively low temperatures (250−400 °C) of calcination crystallizes as Nb_2O_5. The latter is well confirmed by the XPS analysis, while much more stable NbO_2 appears above 900 °C. Such XP spectral experimental evidence reveals the fifth hydroxide (OH^-) ion for the most easily transferable by the membrane type surface and bulk migration within the overall spillover mechanism[6,45]

$$Nb(OH)_5 + Pt \Leftrightarrow Nb(OH)_4^+ + Pt{-}OH + e^- \quad (7)$$

Meanwhile, XPS analysis has also revealed a further interrelating mechanism of similar exchanges with hydrated anatase titania

$$Nb(OH)_4^+ + Ti(OH)_4 \Rightarrow Nb(OH)_5 + Ti(OH)_3^+ \quad (8)$$

or, when summed up

$$Ti(OH)_4 + Pt \Leftrightarrow Ti(OH)_3^+ + Pt{-}OH + e^- \quad (1A)$$

Then, the entire formalism clears up the equivalence and mutual facilitation between titania and niobia for the primary oxide spillover, as already concluded.[6,45]

The conclusive observation from above XPS experimental evidence then has been that such membrane type ionic migration, both through the bulky network and over hypo-d-oxide surface exposure, ending up with the Pt−OH (Au−OH) spillover, is interdependent and can be further remarkably optimized by the common catalyst interactive support structure, in particular by hypo-f-oxide (CeO_2, GdO_2, HoO_2) ingredients with much larger and, hence, much more exposed (and thereby easier interactive and migrating) latent storage hydroxide structure. Let us then add the straight intimate and much more expanded interactive Pt catalyst hydrated interface ($Pt/Nb(OH)_5$, $Ti(OH)_4$, $Ce(OH)_4$) contact and even direct interaction of NaOH from rich alkaline media[30]

$$OH^- + Pt \Leftrightarrow Pt - OH + e^- \quad (9)$$

which is the same and equivalent to eq 1,[30] to become aware of the multiple membrane type migration and even direct spillover Pt−OH generation. In such an electrocatalytic constellation, surface and bulk migration represent now the main overall RDS and afforded open optimization area to provide already superior, broad range reversible electrocatalysts for oxygen electrode reactions (ORR, OER).

XP spectra belong to newer, very reliable, and sophisticated indicative methods enabling some unique conclusive theoretical and practical observations and relations, as the ones just displayed and discussed. Meanwhile, since ultrahigh vacuum ($\leq 10^{-9}$) instantaneously removes all water molecules from the catalyst network and the interphase, while in the present study, the Ertel self-catalytic water molecule contribution is in particular inferred, associated

DOI: 10.1021/jp510234f
J. Phys. Chem. C 2015, 119, 11267−11285

with the Pt−OH spillover, and the whole story is complementary to the others throughout, to rely on, but being incomplete for itself.

The reversible fast adsorptive interacting primary oxides (M−OH) lead up to adsorbed monolayers (Pt−OH → 1) and are distinctly marked by specific potentiodynamic peaks, as the first step of water oxidation (eqs 1 and 2),[2−4] immediately after the initial classical double-layer charging range of many metals, first of all on Ru, Au, Pt, Rh, Ag, and Ni. Similar behavior is exhibited by some other types of transition metal primary oxides of common formulas and structure, like MoO(OH), NiOOH, AuOOH, and WO_2(OH), and can be and have been identified by corresponding peaks within their potentiodynamic and XPS spectra.[32,40] All hypo-d-elements, in particular of high altervalent capacity, afford the reversible primary oxide type states, usually of pronounced catalytic activity and even unusually high electronic conductive properties (WO(OH), MoO_2(OH)), but unfortunately, in their oxidation sequences end-up with nonconductive and catalytically inactive higher valence oxide states (MoO_3, WO_3, Pt═O, PtO_2, Au═O, NiO_2); otherwise, the whole aqueous electrochemistry would feature another and quite different physiognomy!

Striking Electrocatalytic Conclusions. Classical potentiodynamic spectra in aqueous media (Figure 1), straight after the reversible adsorptive Pt−OH peak, reveal unusual, anomalous, longer, and stronger anodic polarization even within the thermodynamic equilibrium potential values ($\Delta E = \Delta E_0 + \eta_r + \eta_a$) and, from the same causes and reasons, along the reverse cathodic sweep, too (Pt−OH → 0, Pt═O → 1). Since the entire amount of reversibly adsorptive Pt−OH, within the same reversible peak and/or the same reversible potential range, undergoes complete disproportionation into the highly polarizable and irreversibly deposited Pt═O monolayer (eq 2), and thereby becomes unavailable for further reaction within such longer (about 600 mV·s^{-1}) potential scans, as a result, there imposes the typical pronounced reaction polarization (η_r), which suppresses further proceeding of the interfering Pt−OH/Pt═O reversible reaction (eq 3), within both, back and forth, scan directions. The latter extends further by the activation polarization (η_a), and all together they impose very strong and broad polarizable properties (Figure 1). On the contrary, interactive (SMSI) supports of mixed valence hypo-d−d−(f)-oxides, *a priori*, behave as continuously renewable and recoverable enormous (Pt−OH) latent storage capacities and spillover sources (Scheme 1) all along the potential range between oxygen and hydrogen evolving limits. Thus, there is now no reaction polarization ($\eta_r = 0$), and since the OER occurs straight from the enormous broad Pt−OH peak, and thereby exactly at the thermodynamic ROE value ($\Delta E_0 = 1.29$ V, $\eta_r = \eta_a = 0$), the reversible electrocatalysts of various interactive hypo-d−(f)-oxide support compositions for oxygen electrode reactions (ORR, OER) have now, finally, been substantiated and tested on Pt and Au. The present conclusive discussion strongly asserts, implies, and reveals why plain, nonmodified Pt by any means can ever become a reversible electrocatalyst for the oxygen electrode reactions, or at least not within the whole potential range between hydrogen and oxygen evolving limits (Figures 1, 3, and 4).

The interplay of interconnected and interrelated potentiodynamic spectra (Figure 1−4), as the ones of main electrochemical tools, have been thoroughly employed to investigate and define spillover phenomena and overall behavior of the primary oxide (Pt−OH), in particular relative to the polarizable surface Pt═O (Au═O) oxide, and reveal therefrom the appearance of the strong reaction polarization range and barrier, as the prevailing effect of unavoidable broader irreversibility features of plain Pt (Au) along the potential axis between hydrogen and oxygen evolving limits. Various individual and/or better mixed valence of altervalent and strong interactive (SMSI) hypo-d−(f)-oxides, as the complementary catalytic supports, have been broadly introduced as the counterbalancing composite species able to suppress and effectively eliminate the polarization impacts, by enriched latent storage for the Pt−OH (Au−OH) spillover, and achieve provided and long lasting reversible electrocatalysts for the oxygen electrode (primarily the ORR) reactions. The entire approach has been based on intermetallic d−d-, d−f-, and f−f-interelectronic bonding features and correlations and consequently reflects extra high stability, advanced electron conductivity, and superior (electro)catalytic features and activity.

The properly conceived potentiodynamic spectral interplay of three complementary different cyclic voltammograms, as the main electrochemical tools, have been confirmed for the reliable system to investigate spillover phenomena and define compatible electrocatalysts for partially, but strongly and broadly polarizable, electrode reactions and then provide novel advanced electrocatalysts for the entire scanning and applied cycle. In such a respect the best hyper-d-electrocatalyst because of *a priori* advanced individual Ru−OH spillover features would be PtRu (AuRu is not yet tested and optimized), insofar best optimized hypo-d−f-interactive supports (Nb_2O_5, Ta_2O_5, and WO_3, in combination with prevailing anatase (101) titania, TiO_2, and at least doped by CeO_2, GdO_2, HoO_2 mixed and altervalent composites). The primary oxide spillover interference between Ru, relative to Pt, the authors infer on, and mixed valence hypo-d−d-oxides, mostly advanced by Nb_2O_5, Ta_2O_5, and WO_3, and promoted by hypo-f-oxide (CeO_2, GdO_2, HoO_2) ingredients, bring the overall electrocatalytic activity to remarkable higher values at higher current densities and mark the general way and manner of their further optimization.[59−77]

All interrelating steps considered, described, and carried out in the course of development of interactive hypo-d−d−(f)-oxide supported electrocatalysts for the OER have substantially been based on the d−d−(f)-ties and bonding strengths and d−(f)-electronic density of states, since the d-band is stated and proved to be cohesive, adsorptive, and catalytic orbital. When stated about their extra high stability in both acidic and alkaline media,[5] this implies primarily metallic properties even of hypo-d−(f)-oxides, first of all as pronounced metallic type of high electron conductivity and with overall intermetallic strengths, features, and behavior. This is the substance in the advanced reversible oxygen electrode electrocatalysis.

AUTHOR INFORMATION

Corresponding Author

*Jelena M. Jaksic. E-mail: jelena@iceht.forth.gr. Phone: +30-2610-435754.

Notes

The authors declare no competing financial interest.

DOI: 10.1021/jp510234f
J. Phys. Chem. C 2015, 119, 11267−11285

Biographies

Dr. Jelena M. Jakšić graduated from Faculty of Physical Chemistry, Faculties of Sciences, University of Belgrade, 1995, with two academic years of studies at Departments of Physics and Chemical Engineering, University of Patras in Greece. Diploma thesis with Professor S. Mentus on Non-Faradaic Electrochemical Modification of Catalytic Activity (NEMCA) for Heterogeneous Reaction of Hydrogen Oxidation in Aqueous Media awarded by Belgrade October city prize for creative contributions of youth, 1997. M.S. at the Center for Multidisciplinary Studies, University of Belgrade, Surface State division, 2000, with Professors N. Krstajić, M. Vojnović, N. Ristić on Kinetics of Hydrogen Evolution on Intermetallic Phases and Alloys of Ni, Co and Mo. PhD degree at Faculty of Technology and Metallurgy, University of Belgrade, 2004, with partial fulfillment at Department of Chemical Engineering, University of Patras, Greece within two EU research projects, "Prometheas" and "Apollon", on Kinetics of Electrochemical Hydrogen Evolution and Oxidation Reactions on Mo−Pt Alloys carried out with Professor N. Krstajic; one-year Greek Ministry of Science grant for Ph.D. thesis work with Dr. S. G. Neophytides. Published 26 peer reviewed scientific papers; SCI 420.

Ms. Feihong Nan was born in China where she completed her BEng degree from Kunming University Science & Technology. Feihong Nan moved to Canada in 2006 and received a MAsc degree in Materials Science and Engineering at McMaster University. She is currently in the final stages of completing her PhD degree, also at McMaster University. She has developed expertise in analytical electron microscopy and in particular scanning transmission electron microscopy and electron tomography. Feihong's research interest is structure-properties in nanoscale energy materials, and she published several papers on this subject.

Dr. Georgios Papakonstantinou received his diploma in Chemical Engineering from National Technical University of Athens in 2001 and completed his PhD in Chemical Engineering at the University of Patras in 2010 under the supervisors Prof. C.G. Vayenas, Member of Greek National Academy of Sciences and Arts, Athens, and Dr. S. G. Neophytides studying the CO tolerance of bimetallic and ternary electrocatalysts in Polymer Electrolyte Fuel Cells, and continued working in the same area at the Institute of Chemical Engineering Science and High Temperature Chemical Processes/Foundation of Research and Technology, Hellas (ICEHT/FORTH) in Patras as a postdoc (2010-2011). He continued his studies on electrode processes and degradation phenomena of low and medium temperature polymer electrolyte fuel cells as research fellow at Joint Research Centre - Institute for Energy and Transport (JRC-IET) in Petten, Netherlands. Presently, he is working on the system analysis and optimization of polymer electrolyte water electrolysis at Max Planck Institute − Dynamics of Complex Technical Systems (MPI-DCTS) in Magdeburg, Germany.

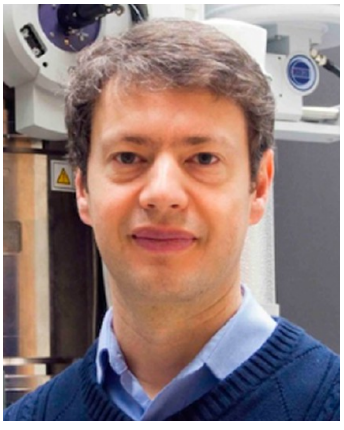

Professor Gianluigi Botton received a degree in Engineering Physics and a PhD in Materials Engineering at Ecole Polytechnique of Montreal. He was Postdoctoral Fellow in the Department of Materials Science and Metallurgy at the University of Cambridge from 1993 to 1998. He joined the Materials Technology Laboratory of Natural Resources Canada (NRCan) in 1998 as a research scientist. In 2001 he moved to the Department of Materials Science and Engineering at McMaster University where he was awarded a Tier 1 Canada Research Chair in Electron Microscopy of Nanoscale Materials. He received the Brian Ives Lectureship of the ASM in 2009 and the CAMBR Lectureship at Western University in 2013 and the NABMM Scientific Merit Award at NRCan. He established, and currently leads, the Canadian Centre for Electron Microscopy, a national facility for ultrahigh-resolution microscopy. His area of expertise is Analytical Electron Microscopy-AEM of nanostructured materials. He is regularly invited to present

DOI: 10.1021/jp510234f
J. Phys. Chem. C 2015, 119, 11267−11285

lectures on the application of microscopy and energy loss spectroscopy (EELS) in catalysts and plasmonics. He wrote five book chapters on microscopy techniques, including the reference on AEM in the Encyclopedia Science of Microscopy (Springer) and on EELS in the book STEM (Springer). He was past president of the Microscopical Society of Canada and he is Editor of Microscopy and on the editorial board of Micron, two international journals dedicated the development and application of microscopy methods.

Professor Milan M. Jaksic graduated in physical chemistry at Faculty of Technology and Metallurgy (TMF), University of Belgrade (1958, grade 9.1/10), and immediately became the Manager of Chlorine and Chlorate Plants (1958−1966), Factory "Jugovinil", near Split, Croatia, where started his doctors thesis and was chosen for the Lecturer in Electrochemical Processes at Faculty of Technology, University of Split (1963). Principal investigator and founder of Laboratory of Industrial Electrochemistry at Center of Electrochemistry, IHTM, Belgrade (1966-78). PhD degree at TMF-UB on Advances in Electrochemical Chlorate Cell Process, with Professor A.R. Despic supervisor, 1970. Fulbright-Huys grantee for postdoc studies in Electrochemical Engineering (Hydrodynamic Effects on Macromorphology of Zinc Electrodeposits and Flow Visualisation) with Professor Charles W. Tobias, at Department of Chemical Engineering and LBL, University of California, Berkeley, 1976−78. Professor in Physical Chemistry at Institute of Food Technology, Faculty of Agriculture, University of Belgrade (1978−2000). Visiting Professorship: (i) University of California, Berkeley with Professor John Newman, 1984; (ii) Laboratory of Industrial Electrochemistry, NTNU, University of Trondheim, Norway, with Professor Reidar Tunold, 1989/90; (iii) Department of Chemical Engineering, and ICEHT/FORTH, University of Patras, Greece with Professor Constantinos G. Vayenas, 1992/94, 2000/01, and on strategic EU projects in PEMFC Electrocatalysis with Dr. Stylianos G. Neophytides, 2001/04, Honored International Affiliated Member at ICEHT/FORTH, 2010 -, www.iceht.forth.gr. Awards: (i) Prestigious October Belgrade city Award, 1974; (ii) "Sir William Grove Award", IAHE (International Association for Hydrogen Energy), for "outstanding contributions to the theory of electrocatalysis for hydrogen electrode reactions", 2006, and (iii) Annual award of Union of University Professors of Serbia, 1999. More than 120 peer reviewed scientific papers mostly in electrocatalysis for oxygen and hydrogen electrode reactions, SCI about 4,000, sharply growing previous six months. EU Expert for Electrocatalysis, 2010-.

■ ACKNOWLEDGMENTS

The present paper has been carried out in the Institute of Chemical Engineering Science, ICEHT/FORTH, Patras, Greece

■ REFERENCES

(1) Grove, W. R. On a Gaseous Voltaic Battery. *Philos. Mag.* **1842**, *21*, 417−420.
(2) Conway, B. E. Electrochemical Oxide Film Formation at Noble Metals as a Surface-Chemical Process. *Prog. Surf. Sci.* **1995**, *49*, 331−452.
(3) Angerstein-Kozlowska, H.; Conway, B. E.; Sharp, W. B. A. The Real Condition of Electrochemically Oxidized Platinum Surfaces: Part I. Resolution of Component Processes. *J. Electroanal. Chem.* **1973**, *43*, 9−36.
(4) Jaksic, J. M.; Krstajic, N. V.; Vracar, Lj. M.; Neophytides, S. G.; Labou, D.; Falaras, P.; Jaksic, M. M. Spillover of Primary Oxides as a Dynamic Catalytic Effect of Interactive Hypo-d-Oxide Supports. *Electrochim. Acta* **2007**, *53*, 349−361.
(5) Jaksic, M. M.; Botton, G. A.; Papakonstantinou, G. D.; Nan, F.; Jaksic, J. M. Primary Oxide Latent Storage and Spillover Enabling Electrocatalysts with Reversible Oxygen Electrode Properties and the Alterpolar Revertible (PEMFC versus WE) Cell. *J. Phys. Chem. C* **2014**, *118*, 8723−8746.
(6) Papakonstantinou, G. D.; Jaksic, J. M.; Labou, D.; Siokou, A.; Jaksic, M. M. Spillover Phenomena and Their Striking Impacts In Electrocatalysis for Hydrogen and Oxygen Electrode Reactions. *Adv. Phys. Chem.* **2011**. *2011*, 1−22, Article ID 412165.
(7) Ma, Y.; Balabuena, P. B. Designing Oxygen Reduction Catalysts: Insights from Metalloenzymes. *Chem. Phys. Lett.* **2007**, *440*, 130−133.
(8) Brewer, L. Bonding and Structures of Transition Metals. *Science* **1968**, *161*, 115−122.
(9) Jaksic, M. M. Hypo-Hyper-d-Electronic Interactive Nature of Synergism in Catalysis and Electrocatalysis for Hydrogen Reactions. *Electrochim. Acta* **2000**, *45*, 4085−4099.
(10) Tauster, S. J.; Fung, S. C.; Baker, R. T. K.; Horsley, J. A. Strong-Interactions in Supported-Metal Catalysts. *Science* **1981**, *211*, 1121−1125.
(11) Vittadini, A.; Selloni, A.; Rotzinger, F. P.; Gratzel, M. Structure and Energetics of Water Adsorbed at TiO_2 Anatase (101) and (001) Surfaces. *Phys. Rev. Lett.* **1998**, *81*, 2954−2957.
(12) Lazzeri, M.; Vittadini, A.; Selloni, A. Structure and Energetics of Stoichiometric TiO_2 Anatase Surfaces. *Phys. Rev. B* **2001**, *63*, No. 155409.
(13) Livage, J.; Henry, M.; Sanchez, C. Sol-Gel Chemistry of Transition Metal Oxides. *Prog. Solid State Chem.* **1988**, *18*, 259−341.
(14) Koper, M. T. M.; Van Santen, R. A. Interaction of H, O and OH with Metal Surfaces. *J. Electroanal. Chem.* **1999**, *472*, 126−136.
(15) Awaludin, Z.; Moo, J. G. S.; Okajima, T.; Ohsaka, T. TaOx − Capped Pt Nanoparticles as Active and Durable Electrocatalysts for Oxygen Reduction. *J. Mater. Chem. A* **2013**, *1*, 14754−14765.
(16) Fugane, K.; Mori, T.; Ou, D. R.; Yan, P.; Ye, F.; Yoshikawa, H.; Drennan, J. Improvement of Cathode Performance on Pt-CeO_x by Optimization of Electrochemical Pretreatment Conditions for PEMFC Application. *Langmuir* **2012**, *28*, 16692−16700.
(17) Volkening, S.; Bedurftig, K.; Jacobi, K.; Wintterlin, J.; Ertl, G. Dual Path Mechanism for Catalytic Oxidation of Hydrogen on Platinum Surface. *Phys. Rev. Lett.* **1999**, *83*, 2672−2675.
(18) Date, M.; Haruta, M. Moisture Effect on CO Oxidation over Au/TiO_2 Catalyst. *J. Catal.* **2001**, *201*, 1221−1224.
(19) Kohn, H. W.; Boudart, M. Reaction of Hydrogen with Oxygen Adsorbed on a Platinum Catalys. *Science* **1964**, *145*, 149−150.
(20) Benson, J. E.; Kohn, H. W.; Boudart, M. On the Reduction of Tungsten Trioxide Accelerated by Platinum and Water. *J. Catal.* **1966**, *5*, 307−313.
(21) Krstajic, N. V.; Vracar, Lj. M.; Radmilovic, V. R.; Neophytides, S. G.; Labou, D.; Jaksic, J. M.; Tunold, R.; Falaras, P.; Jaksic, M. M. Advances in Interactive Supported Electrocatalysts for Hydrogen and Oxygen Electrode Reactions. *Surf. Sci.* **2007**, *601*, 1949−1966.
(22) Mavrikakis, M.; Stoltze, P.; Norskov, J. K. Making Gold Less Noble. *Catal. Lett.* **2000**, *64*, 101−106.
(23) Hammer, B.; Norskov, J. K. Why Gold is the Noblest of all the Metals. *Nature* **1995**, *376*, 238−240.

DOI: 10.1021/jp510234f
J. Phys. Chem. C 2015, 119, 11267−11285

(24) Quaino, P.; Luque, N. B.; Nazmutdinov, R.; Santos, E.; Schmickler, W. Why is Gold such a Good Catalyst for Oxygen Reduction in Alkaline Media? *Angew. Chem., Int. Ed.* **2012**, *51*, 1−5.
(25) Haruta, M. When Gold is not Noble: Catalysis by Nanoparticles. *Chem. Rec.* **2003**, 75−87.
(26) Lina, C.; Song, Y.; Cao, L.; Chen, S. Oxygen Reduction Catalyzed by Au-TiO_2 Nanocomposites in Alkaline Media. *ACS Appl. Mater. Interfaces* **2013**, *5*, 13305−13311.
(27) Jaksic, M. M. Advances in Electrocatalysis for Hydrogen Evolution in the Light of the Brewer-Engel Valence-Bond Theory. *J. Mol. Catal.* **1986**, *38*, 161−202.
(28) Friedel, J.; Sayers, C. M. On the Role of d-d-Electron Correlations in the Cohesion and Ferromagnetism of Transition Metals. *J. Phys. (Paris)* **1977**, *38*, 697−705.
(29) Gschneidner, K. A. Physical Properties and Interrelations of Metallic and Semimetallic Elements. In *Solid State Physics, Advances in Research and Applications*, Seitz, F.; Turnbull, D., Eds.; Academic Press: New York, 1964; Vol. *16*, pp 275−427.
(30) Neophytides, S. G.; Zafeiratos, S.; Jaksic, M. M. Selective Interactive Grafting of Composite Bifunctional Electrocatalysts for Simultaneous Anodic Hydrogen and CO Oxidation. I. Theoretical Concepts and Embodiment of Novel Type Composite Catalysts. *J. Electrochem. Soc.* **2003**, *150*, E512−E526.
(31) Neophytides, S. G.; Murase, K.; Zafeiratos, S.; Papakonstantinou, G.; Paloukis, F. E.; Krstajic, N. V.; Jaksic, M. M. Composite Hypo-Hyper-d-Intermetallic Phases as Supported Interactive Electrocatalysts. *J. Phys. Chem. B* **2006**, *110*, 3030−3042.
(32) Zafeiratos, S.; Papakonstantinou, G.; Jaksic, M. M.; Neophytides, S. G. The Effect of Mo Oxides and TiO_2 Support on the Chemisorption Features of Linearly Adsorbed CO on Pt Crystallites: An Infrared and Photoelectron Spectroscopy Study. *J. Catal.* **2005**, *232*, 127−136.
(33) Jaksic, J. M.; Labou, D.; Papakonstantinou, G. D.; Siokou, A.; Jaksic, M. M. Novel Spillover Interrelating Reversible Electrocatalysts for Oxygen and Hydrogen Electrode Reactions. *J. Phys. Chem. C* **2010**, *114*, 18298−18312.
(34) Neophytides, S. G.; Zafeiratos, S.; Papkonstantinou, G. D.; Jaksic, J. M.; Paloukis, F. E.; Jaksic, M. M. Extended Brewer Hypo-Hyper-d-Interionic Bonding Theory. I. Theoretical Considerations and Examples for Its Experimental Confirmation. *Int. J. Hydrogen Energy* **2005**, *30*, 131−147.
(35) Neophytides, S. G.; Zafeiratos, S.; Papkonstantinou, G. D.; Jaksic, J. M.; Paloukis, F. E.; Jaksic, M. M. Extended Brewer Hypo-Hyper-d-Interionic Bonding Theory. II. Strong Metal-Support Interaction Grafting of Composite Electrocatalysts. *Int. J. Hydrogen Energy* **2005**, *30*, 393−410.
(36) Stevenson, S. A. *Metal-Support Interaction in Catalysis, Sintering and Redispersion*; Van Nostrand: New York, 1987.
(37) Haller, G. L.; Resasco, D. E. Metal−Support Interaction: Group VIII Metals and Reducible Oxides. In *Advances in Catalysis*; Eley, D. D., Pires, H., Weisz, P. B., Eds.; Academic Press: San Diego, 1989; Vol. *36*, pp 173−235.
(38) Jaksic, M. M. Volcano Plots along the Periodic Table, Their Causes and Consequences on Electrocatalysis for Hydrogen Electrode Reactions. *J. New Mater. Electrochem. Syst.* **2000**, *3*, 153−168.
(39) Methfessel, M.; Hennig, D.; Schefler, M. Trends of the Surface Relaxations, Surface Energies, and Work Functions of the 4d Transition Metals. *Phys. Rev. B* **1992**, *46*, 4816−4829.
(40) Jaksic, J. M.; Vracar, Lj. M.; Neophytides, S. G.; Zafeiratos, S.; Papakonstantinou, G. D.; Krstajic, N. V.; Jaksic, M. M. Structural Effects on Kinetic Properties for Hydrogen Electrode Reactions and CO Tolerance along Mo-Pt Phase Diagram. *Surf. Sci.* **2005**, *598*, 156−173.
(41) Jaksic, M. M.; Lacnjevac, C. M.; Grgur, B. N.; Krstajic, N. V. Volcano Plots along Intermetallic Hypo-Hyper-d-Electronic Phase Diagrams and Electrocatalysis for Hydrogen Electrode Reactions. *J. New Mater. Electrochem. Syst.* **2000**, *3*, 169−182.
(42) Jaksic, J. M.; Radmilovic, V. R.; Krstajic, N. V.; Lacnjevac, C. M.; Jaksic, M. M. Volcanic Periodicity Plots along Transition Series, Hypo-Hyper-d-d-Interelectronic Correlations and Electrocatalysis for Hydrogen Electrode Reactions. *Macedonian J. Chem. Chem. Eng.* **2011**, *30*, 3−18.
(43) Masud, J.; Alam, M. T.; Okajima, T.; Ohsaka, T. Catalytic Electrooxidation of Formaldehyde at Ta_2O_5-Modified Pt Electrodes. *Chem. Lett. Jpn.* **2011**, *40*, 252−254.
(44) Masud, J.; Alam, M. T.; Miah, M. R.; Okajima, T.; Ohsaka, T. Enhanced Electrooxidation of Formic Acid at Ta_2O_5-Modified Pt Electrode. *Electrochem. Commun.* **2011**, *13*, 86−89.
(45) Jaksic, J. M.; Papakonstantinou, G. D.; Labou, D.; Siokou, A.; Jaksic, M. M. Spillover Phenomena in Electrocatalysis for Oxygen and Hydrogen Electrode Reactions. In *New and Future Developments in Catalysis: Hybrid Materials, Composites, and Organocatalysts*; Suib, S. L., Ed.; Elsevier: Amsterdam, Holland, 2013; pp 175−212.
(46) Davies, J. C.; Hayden, B. E.; Pegg, D. J.; Rendall, M. E. The Electro-Oxidation of Carbon Monoxide on Ruthenium Modified Pt(111). *Surf. Sci.* **2002**, *496*, 110−120.
(47) Hashimoto, S.; Matsuoka, H. Prolonged Lifetime of Electrochromism of Amorphous WO_3−TiO_2 Thin Films. *Surf. Interface Anal.* **1992**, *19*, 464−468.
(48) Hashimoto, S.; Matsuoka, H. Lifetime of Electrochromism of Amorphous WO_3-TiO_2 Thin Films. *J. Electrochem. Soc.* **1991**, *138*, 2403−2408.
(49) Engelhard, M.; Baer, D. Third Row Transition Metals by X-ray Photoelectron Spectroscopy. *Surf. Sci. Spectra* **2000**, *7*, 1−68.
(50) Siokou, A.; Ntais, S. Towards the Preparation of Realistic Model Ziegler-Natta Catalysts: XPS Study of the $MgCl_2$/$TiCl_4$ Interaction with Flat SiO_2/Si(1 0 0). *Surf. Sci.* **2003**, *540*, 379−388.
(51) Fuentes, R. E.; Garcia, B. L.; Weidner, J. W. A Nb-Doped TiO_2 Electrocatalyst for Use in Direct Methanol Fuel Cells. *ECS Trans.* **2008**, *12*, 239−248.
(52) Bokhimi; Morales, A.; Novaro, O.; Lopez, T.; Sanchez, E.; Gomes, R. Effect of Hydrolysis Catalyst on the Ti Deficiency and Crystallite Size of Sol-Gel-TiO_2 Crystalline Phases. *J. Mater. Res.* **1995**, *10*, 2788−2796.
(53) Suh, M.; Bagus, P. S.; Pak, S.; Rosynek, M. P.; Lunsford, J. H. Reactions of Hydroxyl Radicals on Titania, Silica, Alumina, and Gold Surfaces. *J. Phys. Chem. B* **2000**, *104*, 2736−2742.
(54) Lang, N. D. Theory of Single-Atom Imaging in the Scanning Tunneling Microscope. *Comments Condens. Matter. Phys.* **1989**, *14*, 253−257.
(55) Arbiol, J.; Cerda, J.; Dezanneau, G.; Cirera, A.; Peiro, F.; Cornet, A.; Morante, J. R. Effects of Nb Doping on the TiO_2 Anatase-to-Rutile Phase Transition. *J. Appl. Phys.* **2002**, *92*, 853−861.
(56) Seah, M. P. Quantification of AES and XPS. In *Practical Surface Analysis*, 2nd ed.; Briggs, D., Seah, M. P., Eds.; Wiley: New York, 1990; Vol. *1*, pp 201−256.
(57) Simões, J. A. M.; Beauchamp, J. L. Transition Metal-Hydrogen and Metal-Carbon Bond Strengths: the Keys to Catalysis. *Chem. Rev.* **1990**, *90*, 629−688.
(58) Anderson, L. C.; Mooney, C. E.; Lunsford, J. H. Hydroxyl Radical Desorption from Polycrystalline Palladium: Evidence for a Surface Phase Transition. *Chem. Phys. Lett.* **1992**, *196*, 445−448.
(59) Teichner, S. J. Recent Studies in Hydrogen and Oxygen Spillover and Their Impact on Catalysis. *Appl. Catal.* **1990**, *62*, 1−10.
(60) Rigdon, W. A.; Huang, X. Carbon Monoxide Tolerant Platinum Electrocatalysts on Niobium Doped Titania and Carbon Nanotube Composite Supports. *J. Power Sources* **2014**, *272*, 84−859.
(61) Elezovic, N. R.; Ercius, P.; Kovac, J.; Radmilovic, V. R.; Babic, B. M.; Krstajic, N. V. Synthesis and Characterization of Pt Nanocatalyst on Ru0.7Ti0.3O2 Support as a Cathode for Fuel Cells Application. *J. Electroanal. Chem.* **2015**, *739*, 164−171.
(62) Ting, C.-C.; Liu, C.-H.; Tai, C.-Y.; Hsu, S.-C.; Chao, C.-S.; Pan, F.-M. The Size Effect of Titania-Supported Pt Nanoparticles on the Electrocatalytic Activity Towards Methanol Oxidation Reaction Primarily Via the Bifunctional Mechanism. *J. Power Sources* **2015**, *280*, 166−172.
(63) Antolini, E.; Gonzalez, E. R. Ceramic Materials as Supports for Low-Temperature Fuel Cells Catalysts. *Solid State Ionics* **2009**, *180*, 746−763.

DOI: 10.1021/jp510234f
J. Phys. Chem. C 2015, 119, 11267−11285

(64) Zhang, J.; Vukmirovic, M. B.; Xu, Y.; Mavrikakis, M.; Adzic, R. R. Controlling the Catalytic Activity of Platinum-Monolayer Electrocatalysts for Oxygen Reduction with Different Substrates. *Angew. Chem., Int. Ed.* **2005**, *44*, 2132−2135.
(65) Slavcheva, E.; Borisov, G.; Lefterova, E.; Petkucheva, E.; Boshnakova, I. Ebonex Supported Iridium as Anode Catalyst for PEM Water Electrolysis. *Int. J. Hydrogen Energy* **2015**, DOI: 10.1016/j.ijhydene.2015.03.005.
(66) Kasian, O.; Luk'yanenko, T.; Velichenko, A.; Amadelli, R. Electrochemical Behavior of Platinized Ebonex® Electrodes. *Int. J. Electrochem. Sci.* **2012**, *7*, 7915−7926.
(67) Kasian, O. I.; Luk'yanenko, T. V.; Demchenko, P.; Gladyshevskii, R. E.; Amadellic, R.; Velichenko, A. B. Electrochemical Properties of Thermally Treated Platinized Ebonex® with Low Content of Pt. *Electrochim. Acta* **2013**, *109*, 630−637.
(68) Kasian, O. I.; Luk'yanenko, T. V.; Amadelli, R.; Velichenko, A. B. Electrochemical Properties of Ebonex®/Pt Anodes. *Rus. J. Electrochem.* **2013**, *49*, 557−562; *Elektrokhim.* **2013**, *49*, 627−632.
(69) Lacnjevac, U. C.; Radmilovic, V. V.; Radmilovic, V. R.; Krstajic, N. V. RuOx Nanoparticles Deposited on TiO_2 Nanotube Arrays by Ion-Exchange Method as Electrocatalysts for the Hydrogen Evolution Reaction in Acid Solution. *Electrochim. Acta* **2015**, *168*, 178−190.
(70) Sui, X.; Wang, Z. B.; Xia, Y. F.; Yang, M.; Zhao, L.; Gu, D. M. A Rapid Synthesis of TiO_2 Nanotubes in Ethylene Glycol System by Anodization as Pt-based Catalyst Support for Methanol Electrooxidation. *RSC Adv.* **2015**, DOI: 10.1039/C5RA04112K.
(71) Bejan, D.; Guinea, e.; Bunce, N. J. On the Nature of the Hydroxyl Radicals Produced at Boron-Doped Diamond and Ebonex® Anodes. *Elecctrochim. Acta* **2012**, *69*, 275−281.
(72) Bejan, D.; Malcolm, J. D.; Morrison, L.; Bunce, N. J. Mechanistic Investigation of the Conductive Ceramic Ebonex® as an Anode Material. *Electrochim. Acta* **2009**, *54*, 5548−5556.
(73) Liu, K.; Song, Y.; Chen, S. Defective TiO_2-Supported Cu Nanoparticles as Efficient and Stable Electrocatalysts for Oxygen Reduction in Alkaline Media. *Nanoscale* **2015**, *7*, 1224−1232.
(74) Bates, M. Composite Ni/NiO-$C_{r2}O_3$ Catalyst for Alkaline Hydrogen Evolution Reaction. *J. Phys. Chem. C* **2015**, DOI: 10.1021/jp512311c.
(75) Panek, J.; Kubisztal, J.; Bierska-Piech, B. Ni50Mo40Ti10 Alloy Prepared by Mechanical Alloying as Electroactive Material for Hydrogen Evolution Reaction. *Surf. Interface Anal.* **2014**, DOI: 10.1002/sia.5501.
(76) Wu, Q.; Ruan, J.; Zhou, Z.; Sang, S. Magneli Phase Titanium Suboxide Conductive Ceramic Ti_nO_{2n-} as Support for Electrocatalyst towards Oxygen Reduction Reaction with High Activity and Stability. *J. Cent. South Univ.* **2015**, *22*, 1212−1219.
(77) Zhuang, Y.; Ding, W.; Liu, Y.; Mou, Z.; Sun, J.; Guan, M. Reduced Nanostructured Titanium Oxide Coating as an Electrocatalyst Support for Methanol Oxidation. *J. Cent. South Univ.* **2015**, *50*, 3875−3882.

DOI: 10.1021/jp510234f
J. Phys. Chem. C 2015, 119, 11267−11285